

Field Guide to

Radiometry

Barbara G. Grant

SPIE Field Guides
Volume FG23

John E. Greivenkamp, Series Editor

SPIE
PRESS

Bellingham, Washington USA

Library of Congress Cataloging-in-Publication Data

Grant, Barbara G. (Barbara Geri), 1957-
Field guide to radiometry / Barbara Grant.
p. cm. – (The field guide series ; FG23)
Includes bibliographical references and index.
ISBN 978-0-8194-8827-5
1. Radiation–Measurement. I. Title.
QD117.R3G73 2011
535–dc23

2011033224

Published by

SPIE
P.O. Box 10
Bellingham, Washington 98227-0010 USA
Phone: +1.360.676.3290
Fax: +1.360.647.1445
Email: books@spie.org
Web: <http://spie.org>

Copyright © 2011 Society of Photo-Optical Instrumentation Engineers (SPIE)

All rights reserved. No part of this publication may be reproduced or distributed in any form or by any means without written permission of the publisher.

The content of this book reflects the work and thought of the author. Every effort has been made to publish reliable and accurate information herein, but the publisher is not responsible for the validity of the information or for any outcomes resulting from reliance thereon. For the latest updates about this title, please visit the book's page on our website.

Printed in the United States of America.
First printing



Introduction to the Series

Welcome to the *SPIE Field Guides*—a series of publications written directly for the practicing engineer or scientist. Many textbooks and professional reference books cover optical principles and techniques in depth. The aim of the *SPIE Field Guides* is to distill this information, providing readers with a handy desk or briefcase reference that provides basic, essential information about optical principles, techniques, or phenomena, including definitions and descriptions, key equations, illustrations, application examples, design considerations, and additional resources. A significant effort will be made to provide a consistent notation and style between volumes in the series.

Each *SPIE Field Guide* addresses a major field of optical science and technology. The concept of these Field Guides is a format-intensive presentation based on figures and equations supplemented by concise explanations. In most cases, this modular approach places a single topic on a page, and provides full coverage of that topic on that page. Highlights, insights, and rules of thumb are displayed in sidebars to the main text. The appendices at the end of each Field Guide provide additional information such as related material outside the main scope of the volume, key mathematical relationships, and alternative methods. While complete in their coverage, the concise presentation may not be appropriate for those new to the field.

The *SPIE Field Guides* are intended to be living documents. The modular page-based presentation format allows them to be easily updated and expanded. We are interested in your suggestions for new Field Guide topics as well as what material should be added to an individual volume to make these Field Guides more useful to you. Please contact us at fieldguides@SPIE.org.

John E. Greivenkamp, *Series Editor*
College of Optical Sciences
The University of Arizona

The Field Guide Series

Keep information at your fingertips with all of the titles in the Field Guide Series:

Field Guide to

Adaptive Optics, Robert Tyson & Benjamin Frazier

Atmospheric Optics, Larry Andrews

Binoculars and Scopes, Paul Yoder, Jr. & Daniel Vukobratovich

Diffraction Optics, Yakov Soskind

Geometrical Optics, John Greivenkamp

Illumination, Angelo Arecchi, Tahar Messadi, & John Koshel

Infrared Systems, Detectors, and FPAs, Second Edition, Arnold Daniels

Interferometric Optical Testing, Eric Goodwin & Jim Wyant

Laser Pulse Generation, Rüdiger Paschotta

Lasers, Rüdiger Paschotta

Microscopy, Tomasz Tkaczyk

Optical Fabrication, Ray Williamson

Optical Fiber Technology, Rüdiger Paschotta

Optical Lithography, Chris Mack

Optical Thin Films, Ronald Willey

Polarization, Edward Collett

Radiometry, Barbara Grant

Special Functions for Engineers, Larry Andrews

Spectroscopy, David Ball

Visual and Ophthalmic Optics, Jim Schwiegerling

Introduction

Based on the SPIE bestseller *The Art of Radiometry* by James M. Palmer and Barbara G. Grant, this *Field Guide* provides a practical, hands-on approach to the subject that the engineer, scientist, or student can use in real time. Readers of the earlier work will recognize similar topics in condensed form, along with many new figures and a chapter on photometry.

Written from a systems engineering perspective, this book covers topics in optical radiation propagation, material properties, sources, detectors, system components, measurement, calibration, and photometry. Appendices provide material on SI units, conversion factors, source luminance data, and many other subjects. The book's organization and extensive collection of diagrams, tables, and graphs will enable the reader to efficiently identify and apply relevant information to radiometric problems arising amid the demands of today's fast-paced technical environment.

I gratefully acknowledge the contributions to my education and career from three professors of Optical Sciences at the University of Arizona, gentlemen all. They are the late Jim Palmer (1937–2007), who mentored me in radiometry for many years and provided me the opportunity to complete *The Art of Radiometry*; Emeritus Professor Phil Slater, who selected me as a graduate student and trained me in remote sensing, and who continues to encourage and support me; and Eustace Dereniak, who generously shared his knowledge from the very start, provided me my first opportunities to teach, and has strongly supported my career for more than twenty years. To all, my heartfelt thanks.

This book is dedicated to my family and particularly to the memory of my father, William Grant of Chicago, Illinois, a US Navy veteran of WWII who taught me to play the “Garryowen” as soon as my fingers could reach a piano keyboard.

Barbara G. Grant
September 2011

Table of Contents

Glossary of Symbols and Notation	xi
Introduction to Radiometry	1
The Electromagnetic Spectrum	1
The Basics	2
Propagation of Optical Radiation	3
Plane and Solid Angles	3
Projected Area and Projected Solid Angle	4
$f/\#$ and Numerical Aperture	5
Radiometric Quantities Summarized	6
Photon Quantities	7
Spectral Radiant Quantities	8
Radiance, Radiant Exitance, and Irradiance	9
Exitance–Radiance Relationship	10
Intensity	11
Isotropic and Lambertian Sources	12
Inverse Square Law of Irradiance	13
Cosine ³ and Cosine ⁴ Laws of Irradiance	14
Throughput and Its Invariance	15
Area and Solid Angle Products	16
Basic Radiance and Radiance Invariance	17
The Equation of Radiative Transfer	18
Configuration Factors	19
Power Transfer: Point Source	20
Power Transfer: Extended Source	21
Power Transfer: Field Lens Added	22
Irradiance from a Lambertian Disk	23
Irradiance from a Lambertian Sphere	24
The Integrating Sphere	25
Camera Equation and Image Plane Irradiance	26
Radiometric Properties of Materials	27
Overview of Material Properties	27
Transmission	28
Reflection	29
Absorption and the Conservation of Energy	30
Emission	31
Specular Transmissivity and Reflectivity	32
Single-Surface Illustrations	33
More on Specular Propagation	34

Table of Contents

Transmission: Absorbing and Reflecting Materials	35
Materials as Targets	36
Optical Material Selection Considerations	37
Generation of Optical Radiation	38
Planck's Law	38
Stefan–Boltzmann and Wien Displacement Laws	39
Rayleigh–Jeans Law and Wien Approximation	40
Radiation Laws in Terms of Photons	41
Kirchoff's Law	42
Natural Sources	43
Lambert–Bouguer–Beer Law and Langley Plot	44
Artificial Sources	45
Luminescent Mechanisms	46
Some Luminescent Sources	47
Detectors of Optical Radiation	48
Detector Types	48
Detector Definitions	49
More Detector Definitions	50
Detector Figures of Merit	51
Noise Concepts and Definitions	52
The Most Unpleasant Noises	53
More Unpleasant Noises	54
Thermal Detectors	55
Thermoelectric Detectors	56
The Bolometer	57
Pyroelectric Detectors	58
Photon Detectors	59
Photoconductive Detectors	60
Photoemissive Detectors	61
Photovoltaic Detectors	62
Photovoltaic Current and Performance	63
Detector Interfacing	64
Single and Multiple Detectors	65
Detector Array Architectures	66
Choosing a Detector	67
Radiometric System Components	68
Choppers and Radiation References	68
Baffles and Cosine Correctors	69
Spectral Separation Mechanisms	70

Table of Contents

Prisms and Gratings	71
Filters	72
Calibration and Measurement	73
Radiometric Calibration Basics	73
Radiometric Calibration Philosophy	74
Distant Small Source Calibration	75
Collimators and the Distant Small Source	76
More on Collimators	77
Extended Source Calibrations	78
Other Calibration Methods	79
The Measurement Equation	80
Errors in Measurements	81
Signal-to-Noise Ratio and Measurement Error	82
The Range Equation	83
Radiometric Temperatures	84
Photometry	85
Photometric Quantities	85
Human Visual Response	86
Color	87
Sources and the Eye's Response	88
Appendices	89
SI Base Quantities, Prefixes, and Uncertainty Reporting	89
Physical Constants: 2010 CODATA Recommended Values	90
Source Luminance Values	91
More Source Values	92
Solid Angle Relationships	93
Rays, Stops, and Pupils	94
Diffraction	95
Action Spectra and Optical Radiation Regions	96
Equation Summary	97
References	109
Bibliography	110
Index	112

Glossary of Symbols and Notation

A_p	Projected area
A_s	Source area
AS	Aperture stop
A_{sph}	Sphere surface area
B	Effective noise bandwidth
BLIP	Background-limited infrared photodetector
BRDF	Bidirectional reflectance distribution function
BTDF	Bidirectional transmittance distribution function
c	Velocity of optical radiation in vacuum
C	Coulomb
C	Capacitance
c_1	First radiation constant
c_2	Second radiation constant
CCD	Charge-coupled device
CID	Charge-injection device
CMOS	Complementary metal-oxide semiconductor
CTE	Charge-transfer efficiency
d	Distance
D	Detectivity
D	Entrance pupil diameter
D^*	Specific detectivity
D^{**}	Specific normalized detectivity
D_q^*	Specific detectivity in photons
DQE	Detective quantum efficiency
E	Irradiance
E_f	Fermi level
E_g	Gap energy
E_q	Photon irradiance
E_v	Illuminance
f	Focal length
f	Ratio of port area to integrating sphere area
F	Configuration factor
F	Noise factor
$f/\#$	F-number
$f/\#'$	Working $f/\#$
f_c	Cutoff frequency
F_c	Chopping factor

Glossary of Symbols and Notation

FOV	Field of view
FS	Field stop
f_T	Thermal cutoff frequency
G	Photoconductive gain
G	Radiant power gain
h	Planck's constant
H	Heat capacity
H	Radiant exposure
H_q	Photon exposure
H_v	Photometric exposure
I	Radiant intensity
\bar{i}	Average photocurrent due to mean carrier number
I_{dc}	Direct current
IFOV	Instantaneous field of view
i_n	Noise current
I_q	Photon intensity
i_s	Signal current
I_v	Luminous intensity
j	$\sqrt{-1}$
k	Boltzmann's constant
K	Thermal conductance
K_m	Luminous efficacy (photopic)
K'_m	Luminous efficacy (scotopic)
K_s	1/ f noise source-dependent constant
l	Source maximum linear dimension
L	Radiance
L_q	Photon radiance
LSB	Least significant bit
L_v	Luminance
m	Airmass
m	Grating order number
m	Magnification
M	Radiant exitance
m_p	Pupil magnification
M_q	Photon exitance
M_v	Luminous exitance
n	Number of bits in a digital word
n	Refractive index

Glossary of Symbols and Notation

n	Surface normal vector
N	Mean number of carriers
N	Number of illuminated grating grooves
\bar{n}	Average number of photons
NA	Numerical aperture
ND	Neutral density
NEI	Noise equivalent irradiance
NEP	Noise equivalent power
NF	Noise figure
NP	Entrance pupil
p	Pyroelectric coefficient
P_s	Spontaneous polarization
q	Electronic charge
Q, Q_e	Radiant energy
Q_p, Q_q	Photon energy
Q_{rp}	Resolving power
Q_v	Luminous energy
r	Radius of circle or sphere
R	Range
R	Reflectance factor
R	Resistance
\mathfrak{R}	Responsivity
RA	Resistance-area product
\mathfrak{R}_E	Irradiance responsivity
R_L	Detector load resistance
\mathfrak{R}_L	Radiance responsivity
\mathfrak{R}_q	Photon responsivity
R_T	Thermal resistance
\mathfrak{R}_Φ	Power responsivity
S	Seebeck coefficient
SNR	Signal-to-noise ratio
t	Time
T	Absolute temperature
T	Throughput
T_c	Curie temperature
T_n	Noise temperature
v	Velocity of optical radiation in a medium
V_B	Detector bias voltage
v_j	Johnson noise voltage

Glossary of Symbols and Notation

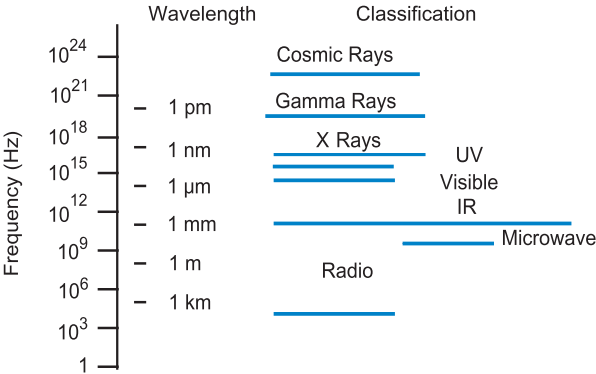
v_n	Noise voltage
v_{rms}	Root-mean-square voltage
V_s, v_s	Signal voltage
$V(\lambda)$	Photopic visual response
$V'(\lambda)$	Scotopic visual response
x	Path length
XP	Exit pupil
X, Y, Z	Tristimulus values based on the 1931 CIE Standard Observer
Z	Impedance
α	Absorptance
α	1/ f noise expression constant
$\alpha'(\lambda)$	Spectral absorption coefficient
β	1/ f noise expression constant
β	Temperature coefficient of resistance (TCR)
ε	Emittance
η	Responsive quantum efficiency
θ	Angle of incidence, reflection, refraction
θ	Angle from normal incidence or emittance
$\Theta_{1/2}$	Half-angle of illumination cone
$\kappa(\lambda)$	Spectral extinction coefficient
λ	Wavelength
λ_0	Wavelength in vacuum
λ_c	Cutoff wavelength
μ	Carrier mobility
Π	Peltier coefficient
ρ	Reflectance
ρ_p	Polarized reflectivity parallel component
ρ_s	Polarized reflectivity perpendicular component
ρ_{ss}	Single-surface reflectance
σ	Standard deviation
σ	Stefan–Boltzmann constant
σ^2	Variance
σ_e	Electrical conductivity
τ	Time constant
τ	Transmittance
$\tau_0(\lambda)$	Spectral optical thickness
τ_{atm}	Atmospheric transmittance

Glossary of Symbols and Notation

τ_i	Internal transmittance
τ_l	Carrier lifetime
τ_{lens}	Lens transmittance
τ_o	Optical transmittance
τ_p	Polarized transmissivity parallel component
τ_s	Polarized transmissivity perpendicular component
τ_{ss}	Single-surface transmittance
τ_T	Thermal time constant
ϕ	Rotational angle
ϕ	Work function in a photoemissive detector
ϕ_0	Potential barrier height in a photovoltaic detector
Φ	Radiant power
Φ_q	Photon flux
Φ_v	Luminous power
ω	Radian frequency ($2\pi f$)
ω	Solid angle
Ω	Projected solid angle
Ω_o	Unit projected solid angle

The Electromagnetic Spectrum

The practical electromagnetic spectrum extends from dc to frequencies greater than 10^{20} Hz. We shall consider the optical portion of the spectrum to cover the five-decade (frequency) range from 3×10^{11} to 3×10^{16} Hz, or roughly 10 nm to 1000 μm (1 mm), and encompasses the ultraviolet, visible, and infrared regions. At shorter wavelengths are x rays, gamma rays, and cosmic rays; at longer wavelengths are microwaves and radio waves.



UVC, UVB, UVA

200 nm–400 nm

Visible

360 nm–780 nm

Near IR

0.78 μm –1.1 μm

Shortwave IR (SWIR)

1.1 μm –2.5 μm

Midwave IR (MWIR)

2.5 μm –7 μm

Longwave IR (LWIR)

7 μm –15 μm

Wavelength regions and subdivisions of the spectrum often overlap and are not always consistent from one authority to another.

Radiation from the far UV through x rays and higher frequencies is called **ionizing radiation**, as it allows an electron to be separated from an atom or molecule.

The Basics

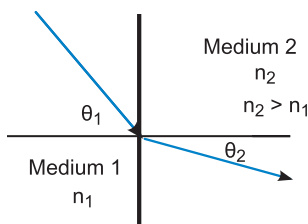
Radiometry is the measurement of optical radiant energy. It also refers more generally to the principles and laws behind the generation, propagation, and detection of optical radiation.

The **velocity of light** c in vacuum is a constant equal to about $3.00 \times 10^8 \text{ ms}^{-1}$, a faster rate of travel than in any other medium. A medium's **refractive index** n is the ratio of c to the **velocity of propagation** v in that medium, $n = c/v$.

Snell's law relates refractive index n to angle of propagation θ within adjacent media due to boundary transition (refraction):

$$n_1 \sin \theta_1 = n_2 \sin \theta_2.$$

When $n_2 > n_1$, the refracted ray travels closer to the boundary normal than does the incident ray. This makes intuitive sense because the sine of a small angle is less than the sine of a larger one when 0- to 90-deg angles are considered.

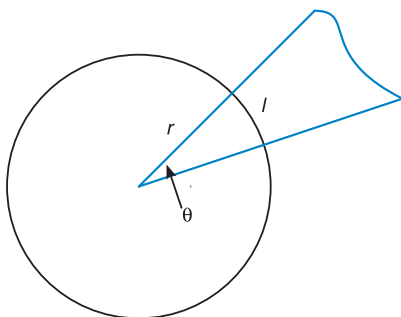


The wavelength of a monochromatic source in a vacuum is related to its wavelength in any medium by $\lambda_0 = n\lambda$.

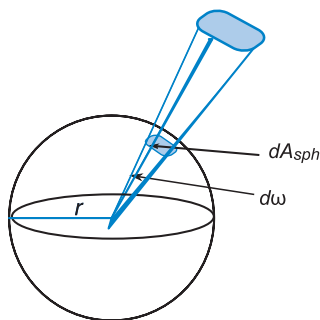
If radiation is outside the visible spectrum, you cannot call it “light.” The visible spectrum extends from about 380 to 760 nm and is perceivable by the normal human eye. Infrared and ultraviolet optical radiation propagate beyond these limits; therefore, there is no such thing as “infrared light” or “ultraviolet light.”

Plane and Solid Angles

Plane angle θ is the angle formed by two radii of a circle. It is defined as the ratio of the arc length to the circle's radius, $\theta = l/r$. Its unit is the radian, the plane angle between two radii of a circle that cut off, on the circumference, an arc equal in length to the radius. There are 2π radians (360 deg) in a circle.



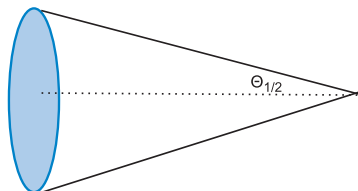
Solid angle ω is the ratio of a subtended spherical surface area to the square of the sphere radius. Its unit is the steradian (sr), the solid angle with vertex at the center of a sphere, subtending an area on the surface of the sphere whose sides have length equal to the sphere radius. The solid angle of a hemisphere is 2π sr, and the solid angle of a sphere is 4π sr.



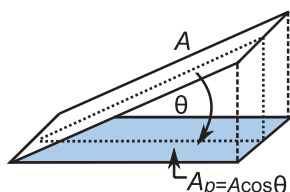
$$d\omega = \frac{dA_{sph}}{r^2} = \sin\theta d\theta d\phi$$

$$\omega = \int_{\phi} \int_{\theta} \sin\theta d\theta d\phi$$

For a right circular cone, $\omega = 2\pi(1 - \cos\Theta_{1/2})$, where $\Theta_{1/2}$ is the cone half-angle.



Projected Area and Projected Solid Angle



Projected area A_p is the rectilinear projection of a surface of any shape onto a plane. In differential form, its expression is $dA_p = \cos \theta dA$, where θ is the angle between the line of observation and the surface normal.

Integrating over the surface area, the expression becomes $A_p = \int_A \cos \theta dA$.

Shape	Surface area	Projected area
Rectangle	$A = LW$	$A_p = LW \cos \theta$
Flat circle	$A = \pi r^2 = \pi d^2/4$	$A_p = \pi r^2 \cos \theta$
Sphere	$A = 4\pi r^2 = \pi d^2$	$A_p = A/4 = \pi r^2$

Projected solid angle Ω is the solid angle ω projected onto the plane of the observer. It may be visualized as the projection of $d\omega$ onto the base of the unit hemisphere. It incorporates an additional cosine term over that in the definition of solid angle.

The projected solid angle of a hemisphere is π sr, and its unit is the steradian.

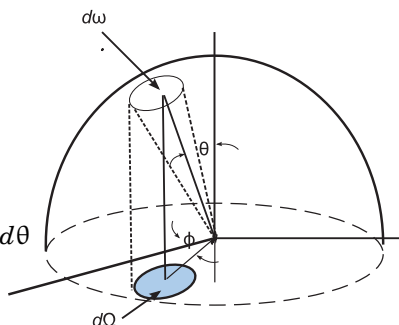
$$d\Omega = \cos \theta d\omega$$

$$= \cos \theta \sin \theta d\theta d\phi$$

For a right circular cone,

$$\Omega = \int_0^{2\pi} d\phi \int_0^{\Theta_{1/2}} \sin \theta \cos \theta d\theta$$

$$= \pi \sin^2 \Theta_{1/2}$$

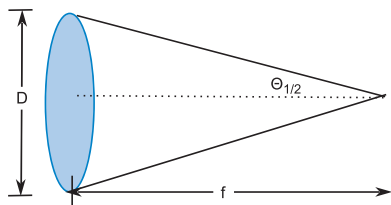


$f/\#$ and Numerical Aperture

The $f/\#$ of an optical system is most often seen defined as the ratio of the effective focal length (object at infinity) of the system to the diameter D of its entrance pupil:

$$f/\# = \frac{f}{D}$$

Good optical systems fulfill the Abbe sine condition, with a spherical wavefront converging to the focal point, and the preferred definition is



$$f/\# = \frac{1}{2 \sin \Theta_{1/2}}$$

This definition implies that $\Omega = \pi / [4(f/\#)^2]$. The two expressions for $f/\#$ are equivalent only **paraxially**, that is, for small values of $\Theta_{1/2}$ such that $\sin \Theta_{1/2} = \tan \Theta_{1/2} = \Theta_{1/2}$.

In cases where image or object are not at infinity, a **working $f/\#$** , $f/\#'$, may be defined as

$$f/\#' = (f/\#)[1 + (m/m_p)]$$

where m_p (the **pupil magnification**) is 1 for a single lens or mirror, and **magnification** m is the ratio of image height to object height.

Numerical aperture (NA) is the sine of the half-angle of the largest axial ray cone that can enter or leave a system, multiplied by the refractive index of the medium in which the cone's vertex is located: $NA = n \sin \Theta_{1/2}$.

Optical designers refer to the $f/\#$ as a measure of the system's speed, but not in the sense of a mechanical scan rate. "Fast" systems gather light more quickly than "slow" systems do; the former have lower $f/\#$ s than the latter.

Radiometric Quantities Summarized

Quantity	Symbol	Definition	Units
Radiant energy	Q or Q_e	—	joule (J)
Radiant power (flux)	Φ	$\frac{dQ}{dt}$	watt (W)
Radiant intensity	I	$\frac{d\Phi}{d\omega}$	W/sr
Radiant exitance	M	$\frac{d\Phi}{dA}$	W/m ²
Irradiance	E	$\frac{d\Phi}{dA}$	W/m ²
Radiance	L	$\frac{d^2\Phi}{dAd\omega\cos\theta}$	W/m ² sr

The above **derived quantities** originate from SI base quantities and are so called by the *Bureau Internationale des Poids et Mesures* and other standards organizations.

Radiant exposure H is defined by NIST as dQ/dA , the derivative of radiant energy with respect to area. It has units of J/m² and is featured in biological applications of light such as phototherapy. It is also defined as $\int E dt$, the integral of irradiance over time. Analogous expressions exist for photon and photometric exposure.

Photon Quantities

Photon quantities are defined analogously to radiometric quantities. They carry the same symbols as radiometric quantities and are subscripted with p or q .

Quantity	Symbol	Definition	Units
Photon energy	Q_q	# photons	—
Photon flux	Φ_q	$\frac{dQ_q}{dt}$	/s
Photon intensity	I_q	$\frac{d\Phi_q}{d\omega}$	/s sr
Photon exitance	M_q	$\frac{d\Phi_q}{dA}$	/s m ²
Photon irradiance	E_q	$\frac{d\Phi_q}{dA}$	/s m ²
Photon radiance	L_q	$\frac{d^2\Phi_q}{dAd\omega\cos\theta}$	/s m ² sr

For easy conversion from W to photons/s at wavelength λ_0 , use $\Phi_q = \Phi \times \lambda_0/hc$, where h is Planck's constant and c is the speed of light in a vacuum.

At $\lambda = 1 \mu\text{m}$, 5.034×10^{18} photons/s = 1 W; and 1 photon has energy $Q = 1.986 \times 10^{-19}$ J. For energy in electron volts (eV), divide Q by the electronic charge q , 1.602×10^{-19} C, to obtain 1.239 eV.

If broadband, integrations must be performed:

$$\Phi_q = \frac{1}{hc} \int_0^\infty \lambda \Phi_\lambda d\lambda \quad \text{and} \quad \Phi = hc \int_0^\infty \left(\frac{\Phi_{\lambda,q} d\lambda}{\lambda} \right)$$

Spectral Radiant Quantities

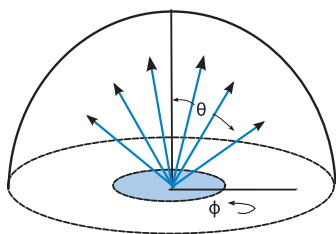
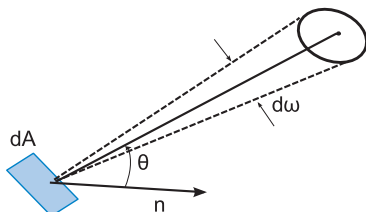
Spectral radiant quantities are defined similarly to their radiometric counterparts and include a derivative with respect to wavelength (or frequency), as though an instrument were able to record the value in an infinitesimally narrow region. This is indicated by the subscript λ . In the table below, the wavelength unit used is meters (m), but the definitions are equally valid for other wavelength units such as nanometers (nm) and micrometers (μm).

Quantity	Symbol	Definition	Units
Spectral radiant energy	Q_λ	$\frac{dQ}{d\lambda}$	J/m
Spectral radiant power	Φ_λ	$\frac{dQ_\lambda}{dt} = \frac{d\Phi}{d\lambda}$	W/m
Spectral radiant intensity	I_λ	$\frac{d^2\Phi}{d\omega d\lambda}$	W/sr m
Spectral radiant exitance	M_λ	$\frac{d^2\Phi}{dAd\lambda}$	W/m ² m
Spectral irradiance	E_λ	$\frac{d^2\Phi}{dAd\lambda}$	W/m ² m
Spectral radiance	L_λ	$\frac{d^3\Phi}{dAd\omega \cos\theta d\lambda}$	W/m ² sr m

The wavelength distribution of a spectral radiant quantity is described as a function of λ , and it is common to see an integration performed over a wavelength band, symbolized as $L_{\Delta\lambda} = \int_{\Delta\lambda} L_\lambda d\lambda$.

Radiance, Radiant Exitance, and Irradiance

Radiance L [$\text{W}/\text{m}^2 \text{ sr}$] is the elemental quantity of radiometry, expressing the power per unit area and per unit projected solid angle from a source; or alternatively, the power per unit projected area per unit solid angle. Radiance is directional in nature, and the sources from which it emanates may be active (a thermal or luminescent emitter) or passive (reflective). As a field quantity, it can be evaluated at any point along a beam in the direction of its propagation.

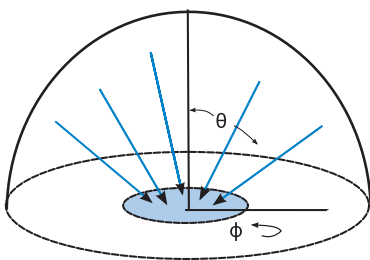


Radiant exitance M [W/m^2] is the power per unit area radiated into a hemisphere; accordingly, it is a measure of flux density.

Mathematically, it may be obtained from radiance by

integrating over the projected solid angle of a hemisphere, π sr: $M = \int_{\pi} L d\Omega$.

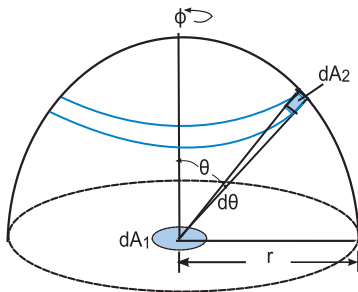
Irradiance E [W/m^2] is the opposite of exitance, as it is the power per unit area from a hemisphere incident upon a surface. Irradiance may be obtained from radiance by integrating over the projected solid angle of a hemisphere, π sr: $E = \int_{\pi} L d\Omega$.



Exitance–Radiance Relationship

The relationship between **radiant exitance** and **radiance** is, in general, complex, and depends greatly on the angular distribution of radiance from the source, $L(\theta, \phi)$.

The power transferred from dA_1 (the source) to dA_2 (on the surface of the sphere) is



$$d^2\Phi = \frac{L(\theta, \phi) dA_1 \cos \theta dA_2}{r^2}$$

where θ is the angle between the surface normal to dA_1 and the direction of propagation. By definition,

$$dA_2 = d\omega \times r^2$$

Substituting for $d\omega$ in terms of θ and ϕ ,

$$dA_2 = r^2 \sin \theta d\theta d\phi$$

Then, the power transferred to the surface dA_2 is

$$d^2\Phi = L(\theta, \phi) dA_1 \sin \theta \cos \theta d\theta d\phi$$

By applying limits for a hemisphere to θ and ϕ , and constructing an integral,

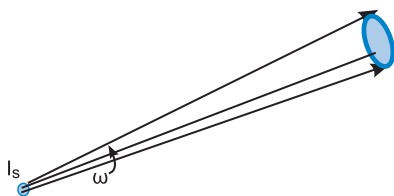
$$\Phi = \int_0^{2\pi} d\phi \int_0^{\pi/2} L(\theta, \phi) A_1 \sin \theta \cos \theta d\theta$$

If the source at A_1 is Lambertian, then

$$\Phi = 2\pi L A_1 \left(\frac{\sin^2 \theta}{2} \right)_0^{\pi/2}$$

Substituting $M = \Phi/A_1$ and solving produces $M = \pi L$; that is, the radiance and radiant exitance of a Lambertian surface are related by a factor of π —the projected solid angle of a hemisphere.

Intensity



Radiant intensity I [W/sr] is the power per unit solid angle emitted from a source. It is associated with a **point source**, one that is small relative to the distance

between the source and target or measurement location. It may be obtained from radiance by integrating over area: $I = \int_A L dA$. Radiant power may be obtained from intensity by integrating over solid angle ω : $\Phi = \int_\omega I d\omega$. For an isotropic point source, the power Φ is 4π , due to the fact that the source radiates uniformly into a sphere of 4π sr.

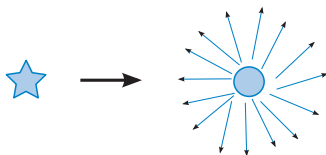
The intensity of a distant star may be determined if we have measurements of its irradiance and distance (the latter can be provided by interferometric techniques).

Intensity is the most frequently misused term in radiometry, used incorrectly to represent quantities including flux density and radiance. “Intensity” and “brightness” are often synonyms in common English usage, but not in radiometry. To avoid confusion, note that (luminous) intensity is an SI base quantity; any reference to the term other than power per unit solid angle is incorrect according to SI terminology.

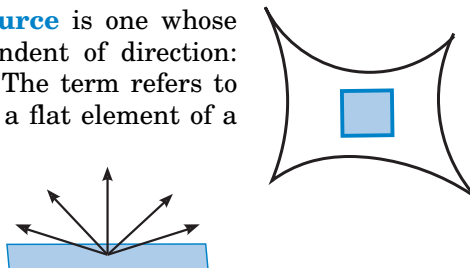
A point source does not exist in reality; if it did, it would have infinite energy density, which is not physically possible. The mathematical construct of a point source simplifies calculations in many circumstances. Yet in this case, as in many others, it is important to make sure that the underlying assumption holds: the source must be suitably distant from the receiver or observation point.

Isotropic and Lambertian Sources

An **isotropic point source** has the same intensity in all directions; this implies a spherical source. A distant star may be considered to approximate an isotropic point source.



A **Lambertian source** is one whose radiance is independent of direction: $L(\theta, \phi) = \text{Constant}$. The term refers to a flat surface or to a flat element of a nonflat surface.



When viewed from a distance, the source radiance and its area projected in the direction of observation comprise its intensity:

$$I = LA_p$$

This intensity falls off as the cosine of the angle between the surface normal and observation direction,

$$I = I_0 \cos \theta$$

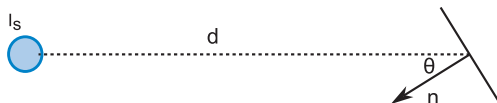
which is **Lambert's law**. A good example of a Lambertian surface is one covered by matte white paint. Under uniform illumination, it appears equally bright from all observation directions.

The Lambertian approximation applies to many different types of surfaces, even to polished metals far from the angle of specular reflection. It is best to confirm this approximation with measurement whenever possible and keep track of its effects on radiometric calculations.

Inverse Square Law of Irradiance

The **inverse square law of irradiance**, one of the most widely used approximations in radiometry, states that the irradiance from an isotropic point source varies inversely with the square of the source distance. In its most general form, it includes the angle between the normal to the receiving (target) surface and the source–receiver axis:

$$E = \frac{I \cos \theta}{d^2}$$

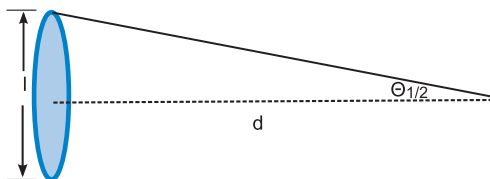


A dimensional analysis of the units on the right-hand side of the equation appears to reveal a discrepancy: while the units of irradiance are W/m^2 , the intensity term provides a per steradian unit as well. A “unit solid angle,” $\Omega_o = 1$ sr, has been proposed, leading to $E = I\Omega_o \cos \theta / d^2$, but the Ω_o term is likely to be confused with a free variable rather than being used as a constant. Instead, it should be remembered that plane and solid angles, being ratios, are dimensionless.

The inverse square law works well for small objects and large distances. Let l be the source’s largest dimension (diameter or length):

- For $l < d/10$ (2.9 deg half-angle), the error in applying the law is $<1\%$.
- For $l < d/20$ (1.4 deg half-angle), the error in applying the law is $<0.1\%$.

If the conditions to apply the inverse square law do not hold, the source must be considered in terms of its area and radiance.



Cosine³ and Cosine⁴ Laws of Irradiance

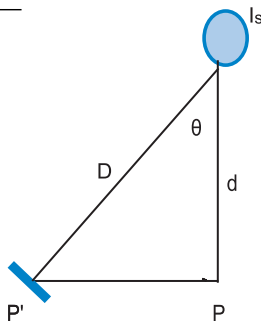


For a target at P oriented toward a point source with intensity I , the irradiance is described by the inverse square law, $E = I/d^2$. If the point P' is drawn a linear distance from P, the irradiance on a target at P' perpendicular to the source is

$$E = \frac{I_s}{D^2} = \frac{I_s \cos^2 \theta}{d^2}$$

If the target is now rotated so that it is parallel to segment PP', another cosine term is applied, and the irradiance at point P' is

$$E = \frac{I_s \cos^3 \theta}{d^2}$$

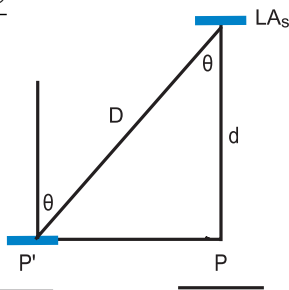
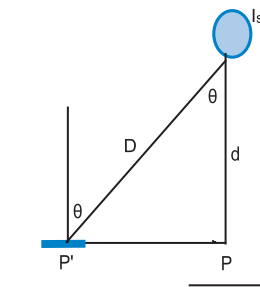


This is the **cosine³ law of irradiance**, valid for an isotropic point source and similar geometry.

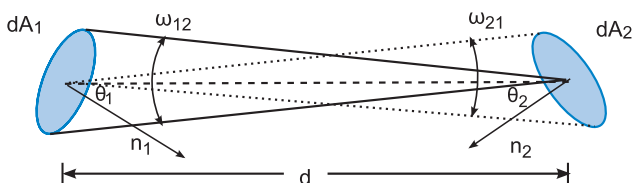
If the point source is replaced by an extended, Lambertian source oriented normal to P, the irradiance at P' must include another cosine term to account for source projection. The extended source must be characterized in terms of its area and radiance as

$$E = \frac{LA_s \cos^4 \theta}{d^2}$$

which is the **cosine⁴ law of irradiance**.



Throughput and Its Invariance

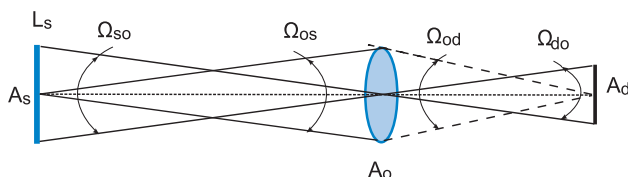


Throughput T , also called *étendue*, geometrical extent, and **$A\Omega$ product**, is the product of the cross-sectional area of a beam and the projected solid angle whose apex is at the areal cross-section and that subtends the next area in the chain. Angles are subscripted so that the first number is the area subtended and the second number is the location of the apex. Therefore, ω_{21} is the solid angle subtended by surface 2 at surface 1. Throughput is invariant within an optical system, $T = A\Omega = \text{Constant}$.

Basic throughput is analogously defined, with the inclusion of the refractive indices of two media on opposite sides of a lossless boundary, $n^2 T = n^2 A\Omega = \text{Constant}$.

The optimal case for throughput analysis arises when the source image entirely fills the detector, there are no transmission losses, and all surfaces are on axis. For that case,

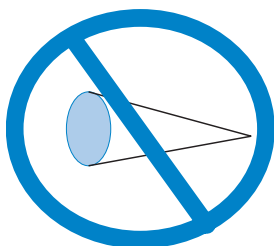
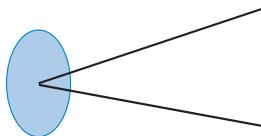
$$A_s \Omega_{os} = A_o \Omega_{so} = A_o \Omega_{do} = A_d \Omega_{od}$$



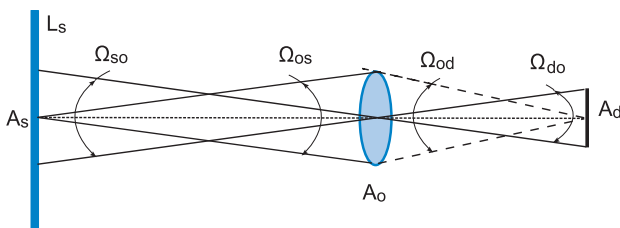
In cases where the paraxial approximation does not apply, a lens must still satisfy the Abbe sine condition for the above relationships to hold.

Area and Solid Angle Products

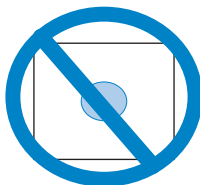
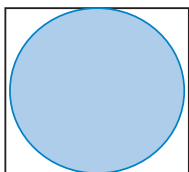
In any analysis of throughput within an optical system, it is important to use the correct **area-solid angle** pair. That pair will always include the angle having its apex at the area under consideration. The maxim “No ice cream cones!” should be applied.



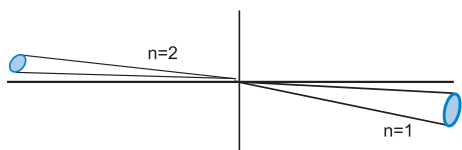
When the source image is larger than the detector (extended source), do not use $A_s\Omega_{os}$ or $A_o\Omega_{so}$, as the radiance from the entire source area will not transfer through the system to reach the detector.



When the source image is smaller than the detector (point source, which may be obtained when viewing the Lambertian area A_s from sufficient distance), do not use $A_d\Omega_{od}$ or $A_o\Omega_{do}$, as the detector area has little meaning when not filled with the source image.



Basic Radiance and Radiance Invariance



If rays are traced along a lossless boundary between two media having different indices of refraction, the solid

angle changes according to Snell's law. Taking this change into account and applying the principle of conservation of energy, the quantity L/n^2 is invariant across the boundary. This quantity is called **basic radiance** and is used when the object and image are located in media with different refractive indices.

Radiance was previously defined as power from a source per unit area and per unit projected solid angle, or alternatively, as power from a source per unit projected area per unit solid angle. The mathematical expressions corresponding to the two cases are

$$L = \frac{d^2\Phi}{dA d\Omega} \quad \text{and} \quad L = \frac{d^2\Phi}{dA_p d\omega}$$

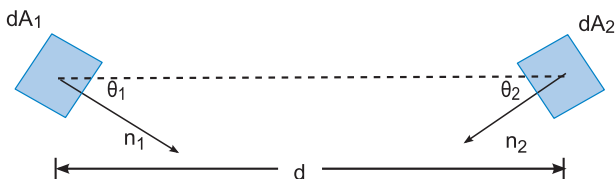
In the absence of sources or sinks along a beam path, and neglecting losses including those due to transmission, reflection, and scattering, power within the beam is conserved. Since throughput is conserved (invariant) in an optical system, radiance must also be invariant in order for conservation of power to be obeyed.

The results of this **radiance invariance** include:

- (1) The radiance of an image at the detector plane of a camera is the same as the radiance of the scene, assuming no transmission losses due to atmosphere and optics; and
- (2) The radiance at the focal plane of a radiometer is the same as that of the target if there are no transmission losses due to atmosphere and optics.

These results greatly simplify radiometric calculations.

The Equation of Radiative Transfer



The **equation of radiative transfer** is arguably the most important equation in radiometry, as it provides the mathematical description for transfer of power (flux) between two surfaces. In differential form, it is

$$d^2\Phi_{1\rightarrow 2} = \frac{L(\theta, \phi)dA_1 \cos \theta_1 dA_2 \cos \theta_2}{d^2}$$

where L is the radiance at surface 1.

In integral form, the equation is

$$\Phi_{1\rightarrow 2} = \int_{A_2} \int_{A_1} \frac{L(\theta, \phi) \cos \theta_1 \cos \theta_2}{d^2} dA_1 dA_2$$

In order to integrate (sum) the incremental contributions to radiant power, the source must be **incoherent** (beam components not in phase) and there must be no interference effects in the beam.

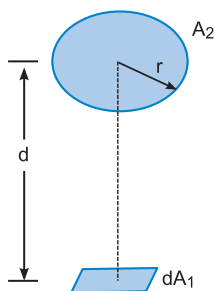
If the following conditions hold, the equation may be simplified:

- Lambertian source so that $L(\theta, \phi)$ is a constant;
- Distance d is much larger than the maximum linear dimension (diameter or length) of A_1 and A_2 ; and
- Both areas are on axis so that θ_1 and θ_2 are zero and their cosines are unity.

If all conditions are met, then

$$\Phi_{1\rightarrow 2} = LA_1\Omega_{21} = LA_2\Omega_{12} = LA\Omega$$

Configuration Factors



Used extensively in heat transfer calculations, **configuration factors** express the geometrical relationships underlying power transfer between two surfaces. The transfer may occur between two differential elements of area, between a differential element and a finite area, or between two finite areas. The major advantage of configuration factors is the existence of many solved geometries easily accessible in print and on-line catalogues. Configuration factor F is defined generally as

$$F = \frac{\Phi_{1 \rightarrow 2}}{\Phi_1}$$

where $\Phi_{1 \rightarrow 2}$ is the power reaching surface 2 from surface 1, and Φ_1 is the power leaving surface 1. It is essential that the source surface be Lambertian; its radiance is L_s . For the case of transfer between two differential area elements, the expression becomes

$$dF_{d_1, d_2} = \frac{\cos \theta_1 \cos \theta_2}{\pi d^2} dA_2 = \frac{1}{\pi} \cos \theta_1 d\Omega_{21}$$

where Ω_{21} is the projected solid angle subtended by surface 2 at surface 1, and the θ_i are the angles between the surface normals and the axis of distance d connecting the two surfaces. The configuration factor relating a differential element and a finite area is

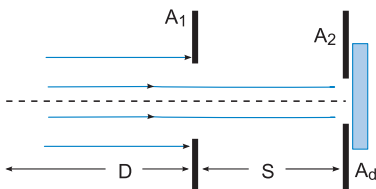
$$F_{d_1, 2} = \int_{A_2} \frac{\cos \theta_1 \cos \theta_2}{\pi d^2} dA_2 = \int_{A_2} dF_{d_1, d_2}$$

If both areas are finite, then

$$F_{12} = \frac{1}{A_1} \int_{A_1} \int_{A_2} \frac{\cos \theta_1 \cos \theta_2}{\pi d^2} dA_2 dA_1 \quad \text{and} \\ \Phi_{1 \rightarrow 2} = L_s A_1 \Omega_{21} = \pi L_s A_1 F_{12} = M_1 A_1 F_{12}$$

Power Transfer: Point Source

In the case of a two-aperture radiometer, with the detector active area defined by aperture area A_2 , and a **point source** at infinity providing a collimated beam, the power on the detector is given by

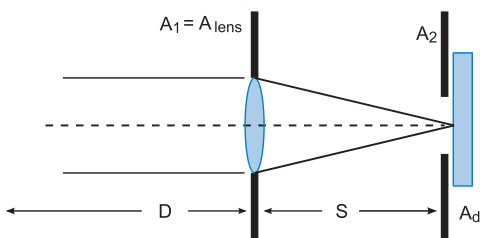


$$\Phi_d = E_d A_2, \quad \text{where } E_d = \frac{I_s}{(D + S)^2}$$

according to the inverse square law of irradiance.

Adding a lens at A_1 causes the beam to focus on the detector, and the power transferred now becomes

$$\Phi_{lens} = E_{lens} A_{lens} = \frac{I_s A_{lens}}{D^2}, \quad \text{with } \Phi_d = \tau_{lens} \Phi_{lens}$$



Assuming that the distance D is large compared to S , the gain in power using a lens is simply the ratio of the areas times the lens transmittance

$$G = \frac{\tau_{lens} A_{lens}}{A_2}$$

For maximum power transfer in this configuration, make τ_{lens} and the area ratio as large as possible, taking care that the image remains fully contained (that is, unvignetted) within A_2 .

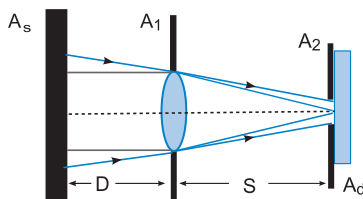
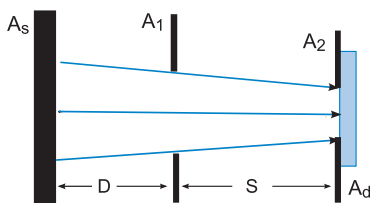
Power Transfer: Extended Source

For an extended source, we use the simplification of the equation of radiative transfer, $\Phi_d = L_s A \Omega$. Because the source is extended, we do not use its area in computation, as that would have no meaning.

At area A_2 , Ω_{12} is the solid angle subtended by area A_1 (notional surface). The equation for power transferred to the detector is

$$\Phi_d = L_s A_2 \Omega_{12} = \frac{L_s A_1 A_2}{S^2}$$

(Note that the same result could be obtained by choosing A_1 as the area.)



The area–solid angle relationship is more precisely illustrated with a lens in place. Again using A_2 and Ω_{12} , the power on the detector is

$$\Phi_d = \tau_{lens} L_s A_2 \Omega_{12} = \frac{\tau_{lens} L_s A_1 A_2}{S^2}$$

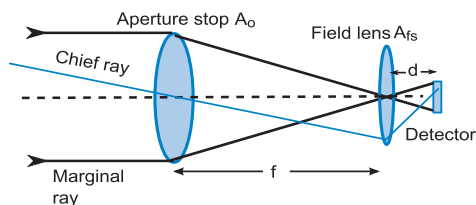
In other words, by placing a lens in the system with an extended source, we have reduced the power on the detector by the transmission of the lens.

The aperture that limits the cone of light entering a system from an on-axis point is called the **aperture stop**. This is A_2 in the case with no lens, and A_1 with a lens. The **field stop** limits the extent the detector can see; it is A_1 in the case with no lens, and A_2 with a lens.

Power Transfer: Field Lens Added

Improvement to the quality of the image may be made by adding a **field lens** to image the aperture stop onto the detector. This approach has several advantages over the lens/detector combination, including uniform irradiance distribution over the detector and the ability to adjust the position of the field lens without changing the position of the detector (the latter being difficult to do, in practice, as the detector assembly includes electronics and other wiring).

In this case, the image of the aperture stop typically underfills or overfills the detector.



$$\Phi_d = L_s A_o \tau_o \Omega_{fs-o} = \frac{\tau_o L_s A_o A_{fs}}{f^2}$$

If it underfills, all power transferred thus far will be transferred to the detector. Optical transmission τ_o is the product of both lens' transmittances.

If it overfills, then

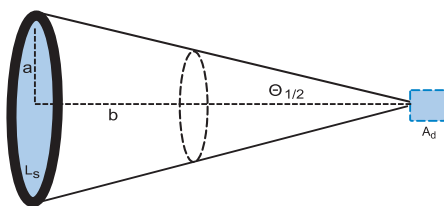
$$\Phi_d = \tau_o L_s A_d \Omega_{fsd} = \frac{\tau_o L_s A_d A_{fs}}{d^2}$$

where d is the distance from the detector to the field stop. If the image of the aperture exactly fills the detector, either expression for power transfer may be used.

A field lens helps control stray radiation within the system. A chopper modulating the input signal may be placed at the field stop and not directly in front of the detector. Multiple detectors sharing a common aperture may be used.

Irradiance from a Lambertian Disk

A common radiative transfer configuration involves a disk and a detector placed on axis so that no cosine terms are needed to describe a projected area. If the disk is **Lambertian**, then the simplification of the equation of radiative transfer can be applied:



$$\Phi_{s \rightarrow d} = L_s A_d \Omega_{sd}$$

The irradiance at the detector is

$$E_d = \frac{\Phi_d}{A_d} = L_s \Omega_{sd} = L_s \pi \sin^2 \Theta_{1/2} = L_s \frac{\pi}{4(f/\#)^2}$$

Expressing relevant quantities in terms of the source-detector distance and source area, we have

$$\sin^2 \Theta_{1/2} = \frac{a^2}{a^2 + b^2} \quad \text{and} \quad E_d = \pi L_s \frac{a^2}{a^2 + b^2}$$

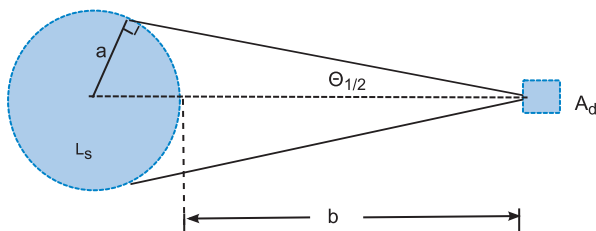
The latter result allows us to calculate the irradiance at the detector for a variety of source–detector distances as we change distance b . This is particularly significant when deciding where to place a source (or detector) for accurate radiometric calibration.

Distance b	Half-angle $\Theta_{1/2}$	Irradiance E_d
$b \gg 2a$	Very small	$\pi L (a^2/b^2), I_s/b^2$
$b = 2a$	26.5	$\pi L/5$
$b = a$	45	$\pi L/2$
$b = 0$	90	πL

If the disk is not Lambertian, radiance is not independent of direction, and integration is required to obtain its value. Closed-form solutions are rare, and numerical integration methods are typically employed for this task.

Irradiance from a Lambertian Sphere

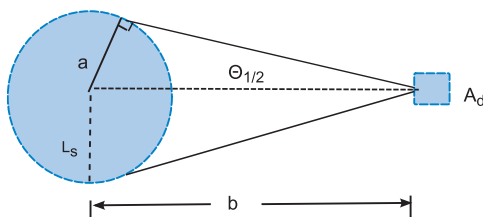
Case I: Sphere surface at distance b from detector:



$$E_d = \pi L a^2 / (a^2 + 2ab + b^2) \quad \sin^2 \Theta_{1/2} = a^2 / (a + b)^2$$

Distance b	Half-angle $\Theta_{1/2}$	Irradiance E_d
$b \gg 2a$	Very small	$\pi L (a^2/b^2), I_s/b^2$
$b = 2a$	19.5	$\pi L/9$
$b = a$	30	$\pi L/4$
$b = 0$	90	πL

Case II: Sphere center at distance b from detector:



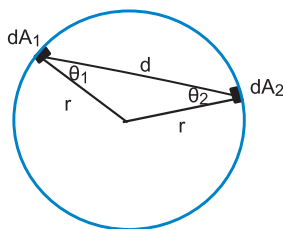
$$E_d = \pi L a^2 / b^2 = L_s A_p / b^2 = I_s / b^2 \quad \sin^2 \Theta_{1/2} = \frac{a^2}{b^2}$$

Distance b	Half-angle $\Theta_{1/2}$	Irradiance E_d
$b \gg 2a$	Very small	$\pi L (a^2/b^2), I_s/b^2$
$b = 2a$	30	$\pi L/4$
$b = a$	90	πL

Notes: (1) At $b \gg 2a$, the source's shape doesn't matter, as it is considered a point source. (2) Case II shows that the inverse square law holds for any **Lambertian sphere** and distance when distance is measured from the sphere's center—mathematically true, but important to measure.

The Integrating Sphere

An **integrating sphere** provides a spatially uniform source of radiance due to multiple reflections from its interior coating (Lambertian). Because r is the sphere radius, $\theta_1 = \theta_2 = \theta$; $\cos \theta = d/2r$. Assume that $dA_1 = dA_2 = dA$. Employing the equation of radiative transfer,



$$d^2\Phi_{1 \rightarrow 2} = \frac{L dA^2 \cos^2 \theta}{d^2} = \frac{L dA^2 d^2}{4r^2 d^2} \quad \text{and} \quad dE = L dA / 4r^2$$

For a Lambertian surface, $L = E\rho/\pi$, so $dE = E\rho dA/4\pi r^2$. This is the irradiance on a small element of area dA . Integration over the interior surface is complex and must take account of multiple reflections. The bottom line is

$$E = \frac{\rho\Phi}{4\pi r^2(1 - \rho)}$$

where Φ is the power on a source placed into the sphere through a port. This irradiance—constant over the sphere by virtue of geometry (dependent only on r) and varying only with small variations in reflectance ρ —makes the sphere a useful radiance source.

Real spheres are fitted with ports and baffles, have nonuniform coatings, and are never exactly Lambertian. The radiance in a practical sphere may be estimated as $L = \rho\Phi/\pi A_{sph}[1 - \rho(1 - f)]$, where f is the ratio of the total port area to that of the sphere. Uses for these spheres include

- Uniform radiance source
- Depolarization
- Light source mixing; color mixing
- Cosine-corrected receivers
- Reflectance and transmittance measurement

Camera Equation and Image Plane Irradiance

The **camera equation** describes image irradiance at the focal plane for a system operating at finite conjugates; m is the magnification.

$$E_t = \frac{\pi L_s}{4(f/\#)^2(1+m)^2}$$

For an object at infinity, $m = 0$ and $E_t = \pi L_s/4(f/\#)^2$. For equal conjugates, $m = 1$ and $E_t = \pi L_s/16(f/\#)^2$.

More general equations for **image plane irradiance**, from extended and point sources respectively, are

$$E_t = \frac{\tau_o \tau_{atm} \pi f_v (1 - A^2) L_s(\theta, \phi) \cos^n \theta}{4(f/\#)^2(1+m)^2} \quad \text{and}$$

$$E_t = \frac{\tau_o \tau_{atm} f_v (1 - A^2) I_s \cos^n \theta}{d^2}$$

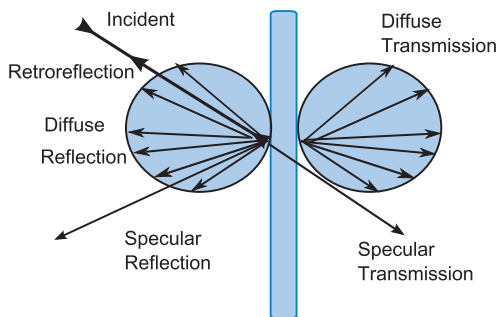
where τ_o is optical transmittance, τ_{atm} is atmospheric transmittance, f_v is a vignetting factor, and $A = (\text{obscuration diameter/primary mirror diameter})$ for centrally obscured systems. The variable n accounts for projections of source and target areas, as discussed previously. It is 3 for an isotropic (point) source and typically 4 for an extended Lambertian source.

Why would the variable n be *typically* 4, rather than always 4, for an extended Lambertian target given the cosine⁴ law? The answer is that good optical designers have been able to reduce n to 3 by deliberately introducing aberrations into certain optical designs.¹ Note that this also points to the importance of specifying *exactly where* irradiance is being calculated. It is best not to “plug and chug!”

Overview of Material Properties

Optical radiation incident upon a boundary between media may be **reflected**, **transmitted**, or **absorbed**, with the process or processes occurring dependent on the wavelength and directional properties of the incoming radiation, and the properties of the material.

Reflectance, transmittance, and absorptance are all ratios of output to input radiometric quantity. This makes them different from radiant power, radiance, irradiance, etc., which are defined in terms of derivatives. The distinction is important, particularly when measurements over a small wavelength region are considered. While the radiant power at a particular wavelength is Φ_λ , the subscript denoting a spectral region as small as the measurement equipment makes possible, the material property $P(\lambda)$ at that wavelength is $P(\lambda) = \Phi_{\lambda o} / \Phi_{\lambda i}$, the subscripts o and i denoting output and input, respectively. Transmittance, reflectance, and absorptance are never actually measured, only calculated.



Considerable debate exists over the suffixes “-ance” and “-ivity” in material properties definition. The usage here reserves terms ending in “-ivity” for the properties of a pure substance (e.g., the reflectivity of pure aluminum, calculated from its complex index of refraction with n and κ vs. the reflectance of a particular specimen of 6061 aluminum with surface structure associated with rolling machining and a natural oxide layer).

Transmission

Transmission is the process by which incident radiant flux leaves a surface or medium from a side other than the incident side (usually the opposite one). **Spectral transmittance** $\tau(\lambda)$ is the ratio of the transmitted spectral flux to the incident spectral flux:

$$\tau(\lambda) = \Phi_{\lambda t} / \Phi_{\lambda i}$$

Total transmittance τ is the transmitted spectral flux weighted by the source function:

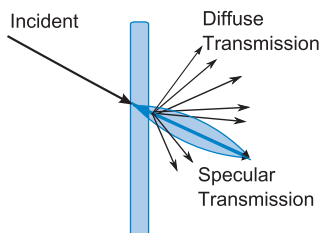
$$\tau = \frac{\Phi_t}{\Phi_i} = \frac{\int_0^\infty \tau(\lambda) \Phi_{\lambda i} d\lambda}{\int_0^\infty \Phi_{\lambda i} d\lambda}$$

Note that total transmittance τ is not $\int_\lambda \tau(\lambda) d\lambda$.

Transmittance may also be described in terms of radiance:

$$\tau = \frac{\int_0^\infty \int_0^{2\pi} L_\lambda^t d\Omega_t d\lambda}{\int_0^\infty \int_0^{2\pi} L_\lambda^i d\Omega_i d\lambda}$$

where L_λ^i is the spectral radiance incident from direction (θ_i, ϕ_i) , L_λ^t is the spectral radiance transmitted to (θ_t, ϕ_t) , and $d\Omega$ is the elemental projected solid angle, $\sin\theta \cos\theta d\theta d\phi$.



Geometrically, transmittance can be classified as specular, diffuse, or total, depending on which direction is named for the emerging signal. Note that the specular transmission direction has a spread to it: it does not occur exactly at one

angle. The **bidirectional transmittance distribution function (BTDF)** relates the transmitted and incident beams as

$$f_t(\theta_i, \phi_i; \theta_t, \phi_t) = \frac{dL_t(\theta_t, \phi_t)}{dE_i(\theta_i, \phi_i)} = \frac{dL_t(\theta_t, \phi_t)}{L_i(\theta_i, \phi_i) d\Omega_i} \text{sr}^{-1}$$

Reflection

In **reflection**, a fraction of the radiation incident upon a surface is returned into the hemisphere above it. Exactly how much is returned, and its directional distribution, are determined by the wavelength and directionality of the incident radiation and the properties of the reflecting surface.

Spectral reflectance $\rho(\lambda)$ is defined analogously to its transmittance counterpart, $\rho(\lambda) = \Phi_{\lambda r} / \Phi_{\lambda i}$, where $\Phi_{\lambda r}$ and $\Phi_{\lambda i}$ represent reflected and incident flux, respectively.

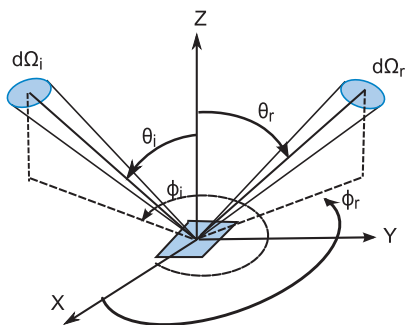
Total reflectance ρ is therefore

$$\rho = \frac{\Phi_r}{\Phi_i} = \frac{\int_0^\infty \rho(\lambda) \Phi_{\lambda i} d\lambda}{\int_0^\infty \Phi_{\lambda i} d\lambda} \text{ and not } \int_\lambda \rho(\lambda) d\lambda$$

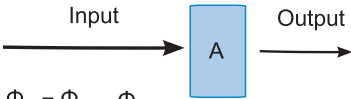
Considerable research has been done on reflectance processes due to their prevalence in many applications of optics and radiometry. The **bidirectional reflectance distribution function (BRDF)** is the fundamental geometric reflectance descriptor:

$$f_r(\theta_i, \phi_i; \theta_r, \phi_r) = \frac{dL_r(\theta_r, \phi_r)}{dE_i(\theta_i, \phi_i)} = \frac{dL_r(\theta_r, \phi_r)}{L_i(\theta_i, \phi_i) d\Omega_i} \text{ sr}^{-1}$$

The equation describes the differential element of reflected radiance dL_r in a specified direction per unit differential element of incident irradiance dE_i in a specified direction. For a perfectly diffuse (Lambertian) surface, the BRDF is ρ/π . For a specular surface, BRDF is ρ/Ω , where Ω is the solid angle the source subtends at the reflective surface.



Absorption and the Conservation of Energy


Absorption is the process by which a fraction of the incident radiant flux is converted to another form of energy, usually heat, and is neither reflected as flux, nor transmitted. **Spectral absorptance** $\alpha(\lambda)$ is defined as $\alpha(\lambda) = \Phi_{\lambda a} / \Phi_{\lambda i}$, with the subscripts denoting absorbed and incident optical power, respectively. **Total absorptance** α is then

$$\Phi_a = \Phi_{in} - \Phi_{out}$$

$$\alpha = \frac{\Phi_a}{\Phi_i} = \frac{\int_0^\infty \alpha(\lambda) \Phi_{\lambda i} d\lambda}{\int_0^\infty \Phi_{\lambda i} d\lambda} \text{ and not } \int_\lambda \alpha(\lambda) d\lambda$$

Absorption removes power from a beam; directional characteristics such as bulk scattering are not often taken into consideration. Due to **conservation of energy**, the sum of transmitted, reflected, and absorbed beam components must be unity:

$$\tau + \rho + \alpha = 1$$

The above statement assumes integration over all wavelengths and directions. In the absence of wavelength-shifting effects (for example, Raman scattering or luminescence), this relationship is also valid for any specific wavelength:

$$\tau(\lambda) + \rho(\lambda) + \alpha(\lambda) = 1$$

Reflectance factor R is the ratio of radiant flux reflected by a particular sample to the radiant flux that would be reflected by a Lambertian surface under the same irradiation conditions. Reflectance factor can be integrated over a particular wavelength band or spectral quantity, $R(\lambda)$. Although reflectance ρ cannot exceed unity, reflectance factor can take on values from 0 to nearly infinity—it is useful as a descriptor for diffuse reflectors but not for other surface types.

Emission

The processes of transmission, reflection, and absorption have a key feature in common: all modify radiation that is propagating. **Emission** is different in this regard, as it is part of radiation generation rather than propagation. As a result, emittance is better defined in terms of radiometric quantities we associate immediately with sources, radiance, or radiant exitance. **Spectral emittance** $\varepsilon(\lambda)$ is the ratio of a source's radiance to that of a blackbody at the same wavelength and temperature:

$$\varepsilon(\lambda) = L_{\lambda(\text{source})} / L_{\lambda BB}$$

Total emittance ε is also weighted by blackbody radiance and is a function of emission direction:

$$\varepsilon = \frac{\iiint \varepsilon(\theta, \phi; \lambda) L_{\lambda BB} \sin \theta \cos \theta d\theta d\phi d\lambda}{(\sigma/\pi)T^4}$$

where σ = the Stefan–Boltzmann constant, and $(\sigma/\pi)T^4$, to be discussed later, is the integrated blackbody radiance at T . Note that total emittance is not $\int_{\lambda} \varepsilon(\lambda) d\lambda$.

One advantage of working with emittance is that it can be equated to absorptance when conditions of thermal equilibrium are met. In that case, $\tau + \rho + \alpha$ becomes $\tau + \rho + \varepsilon$. In the infrared, most materials are opaque, and $\tau = 0$, resulting in $\varepsilon = 1 - \rho$. This relationship greatly simplifies a variety of calculations, given appropriate geometries.

The wavelength-selective ratio α/ε is often employed in coating design, where it is desirable to have a surface that strongly absorbs in one spectral region and weakly emits in another. This is the case in, for example, solar thermal systems used for water and space heating, in which coating absorption at low wavelengths is made as high as possible and emission at longer wavelengths as low as possible.

Specular Transmissivity and Reflectivity

Specular transmissivity and **reflectivity** for a single surface may be calculated from the **Fresnel equations** using the complex index of refraction $n + i\kappa$. (Note the change in terminology [“-ivity”] with reference to a “pure” substance rather than a specific sample.) In the case of no absorption, $\kappa = 0$, the general equations are

$$\begin{aligned}\rho_p &= \frac{(n_2 \cos \theta_1 - n_1 \cos \theta_2)^2}{(n_2 \cos \theta_1 + n_1 \cos \theta_2)^2} \\ \rho_s &= \frac{(n_1 \cos \theta_1 - n_2 \cos \theta_2)^2}{(n_1 \cos \theta_1 + n_2 \cos \theta_2)^2} \\ \tau_p &= \frac{(2n_1 \cos \theta_1)}{(n_2 \cos \theta_1 + n_1 \cos \theta_2)^2 X} \\ \tau_s &= \frac{(2n_1 \cos \theta_1)}{(n_1 \cos \theta_1 + n_2 \cos \theta_2)^2 X}\end{aligned}$$

where the ρ_i are reflectivity, τ_i are transmissivity, and $X = (n_2 \cos \theta_2 / n_1 \cos \theta_1)$. The two polarization states are represented by subscripts p (parallel) and s (perpendicular, from the German word *senkrecht*). From these equations, expressions in terms of θ_1 may be derived using Snell's law and the law of specular reflection relating incident and reflected beams, $\theta_r = \theta_i$.

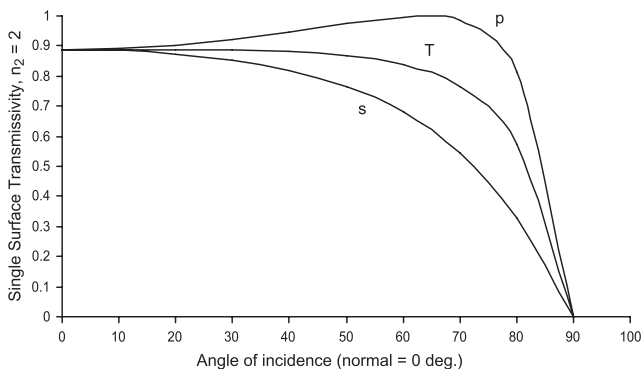
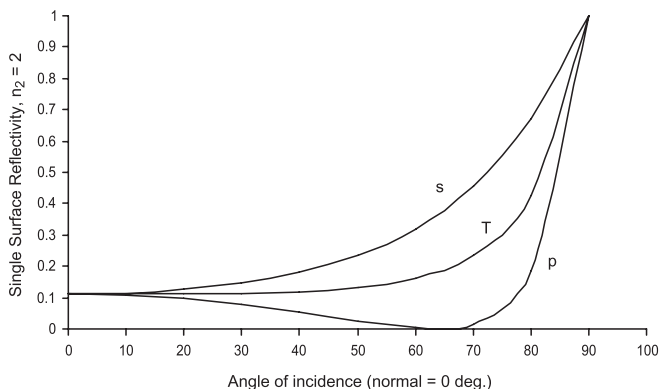
$$\rho_p = \left[\frac{n_1 \sqrt{1 - \left(\frac{n_1}{n_2} \sin \theta_1\right)^2} - n_2 \cos \theta_1}{n_1 \sqrt{1 - \left(\frac{n_1}{n_2} \sin \theta_1\right)^2} + n_2 \cos \theta_1} \right]^2$$

In the non-absorbing case, $\tau_p = 1 - \rho_p$ and $\tau_s = 1 - \rho_s$.

$$\rho_s = \left[\frac{n_1 \cos \theta_1 - n_2 \sqrt{1 - \left(\frac{n_1}{n_2} \sin \theta_1\right)^2}}{n_1 \cos \theta_1 + n_2 \sqrt{1 - \left(\frac{n_1}{n_2} \sin \theta_1\right)^2}} \right]^2$$

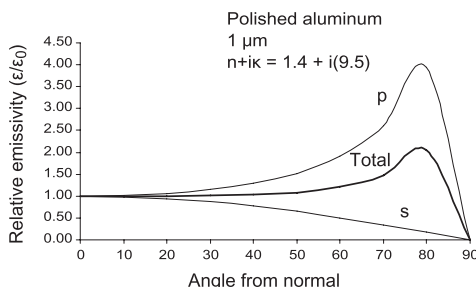
Single-Surface Illustrations

The **total transmissivity** τ_T or **reflectivity** ρ_T for unpolarized light is the average of the parallel and perpendicular components: $\rho_T = (\rho_p + \rho_s)/2$ and $\tau_T = (\tau_p + \tau_s)/2$. Note that these are also called ρ_{ss} and τ_{ss} (**single-surface reflectivity** and **transmissivity**, respectively).



More on Specular Propagation

Normal incidence greatly simplifies calculation with the Fresnel equations, as $\theta_1 = \theta_2 = 0$. For a single surface and non-absorbing medium, they are: $\rho_{ss} = [(n_2 - n_1)/(n_2 + n_1)]^2$ and $\tau_{ss} = (4n_1n_2)/(n_2 + n_1)^2$.



Calculations become more complicated with an absorptive medium. In these cases, the refractive index is the complex quantity

$$n + i\kappa, \kappa(\lambda) = (\lambda/4\pi)\alpha'(\lambda)$$

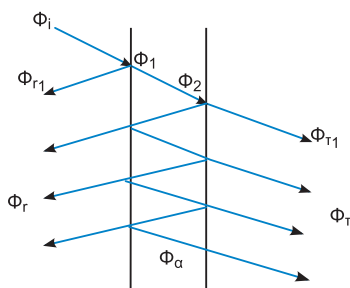
where $\alpha'(\lambda)$ is the material's **spectral absorption coefficient** (per unit length) and $\kappa(\lambda)$ is the **spectral extinction coefficient**. The **internal transmittance** τ_i of a material is described by an exponential absorption relationship, the **Lambert–Bouguer–Beer law**

$$\tau_i(\lambda) = e^{-\alpha'(\lambda)x}$$

where x is the path length. The product $\tau_o(\lambda) = \alpha'(\lambda)x$ is the material's **optical thickness** τ_o at that particular wavelength.

Optical thickness is dimensionless due to the product of cm^{-1} and cm (or μm^{-1} and μm). Optical thickness discussions also apply to the atmosphere, where path length is in km. Spectral absorptance and spectral absorption coefficient are different quantities, the first being a measured power ratio (an “-ance”), and the second a material property needed to calculate an “-ivity.”

Transmission: Absorbing and Reflecting Materials



Real materials have both absorptive and reflective properties; the transmitted radiation will be modified accordingly. For a sample illuminated by unpolarized, collimated radiation, the first-pass quantities are as follows:

First-surface (single-surface) reflection: $\rho_{ss} = \Phi_{r1}/\Phi_i$

First-surface transmission: $\tau_{ss} = \Phi_{t1}/\Phi_i$

Internal transmission: $\tau_i = \Phi_2/\Phi_1 = e^{-\tau_o}$

For an infinite number of passes, the Fresnel equations provide the following relationships:

Transmissivity: $\tau_{\infty} = \frac{(1 - \rho_{ss}^2)\tau_i}{1 - \rho_{ss}^2\tau_i^2}$

Reflectivity: $\rho_{\infty} = \rho_{ss} + \frac{\rho_{ss}(1 - \rho_{ss})^2\tau_i^2}{1 - \rho_{ss}^2\tau_i^2}$

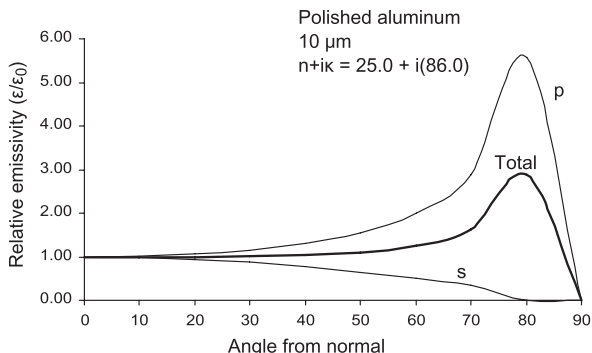
Absorptivity: $\alpha_{\infty} = \frac{(1 - \rho_{ss})(1 - \tau_i)}{1 - \rho_{ss}\tau_i}$

When the optical thickness is large, the material becomes opaque and the transmittance goes to zero. In this case, reflectance ρ approaches the single-surface reflectance ρ_{ss} . When the optical thickness approaches zero, the material becomes transparent. In that case,

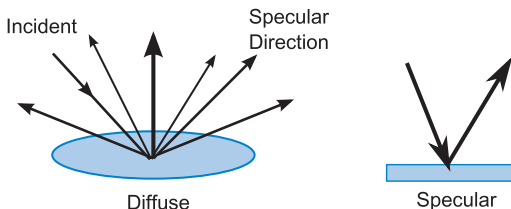
$$\rho = \rho_{ss} + \frac{[\rho_{ss}(1 - \rho_{ss})^2]}{(1 - \rho_{ss}^2)}; \quad \tau = \frac{(1 - \rho_{ss})^2}{(1 - \rho_{ss}^2)}$$

Materials as Targets

Real **targets** (real materials) exhibit a variety of non-ideal directional behavior; specular and Lambertian (perfectly diffuse) are two extremes, but real targets do not reach these limits and often exhibit a mix of both characteristics in varying degrees.



Interestingly, when material transmittance is zero and the index of refraction is complex, a polished metal (aluminum, above) exhibits Lambertian emissivity in the sum of both polarizations out to about 60 deg from normal, though the s - and p -polarization components vary from this. One would seldom consider a polished metal to be Lambertian, and the amount of radiation emitted is low, but angular properties play a significant role.



On the opposite end in terms of emittance values, aluminum, described as “weathered” or “anodized” in the literature, is a diffuse emitter and has comparatively high infrared emittance of 0.83–0.84.

Optical Material Selection Considerations

A system designer selecting optical materials must consider optical, thermal, mechanical, environmental, and other properties of the lenses, mirrors, housing, baffles, etc., used in the design. Many are listed below; not all apply in every case.

Material Properties

Optical

Transmission
Refractive index
Dispersion
Reflection
Sub-surface scatter
Absorption
Homogeneity
Birefringence
Fluorescence
Anisotropy

Thermal

Thermal conductivity
Specific heat
Heat capacity
Coefficient of linear thermal expansion
Softening point
Melting point

Mechanical

Young's modulus
Yield point
Hardness
Optical workability
Coating compatibility
Density, specific gravity

Environmental

Solubility in water or other solvents
Surface deterioration
Radiation susceptibility (space missions)
Behavior in vacuum
Tolerance to vibration

Others

Availability
Safety
Cost

The phenomena that will be measured by the system must be considered, as well. Parameters include the spectral range of the phenomenon, its temperature, and its emittance. Some representative emittance values measured normal to the emitting object in the 8–14 μm region of the infrared are supplied below.

Material	Temperature	Emittance
Polished Al	300 K–900 K	0.03–0.04
Heavily anodized Al	373 K	0.84
Carbon, lampblack	300 K	0.95
Human skin	300 K	0.98
Water	273 K–373 K	0.96

Planck's Law

Any object above 0K will radiate in some relationship to **Planck's law**:

$$L_{\lambda} = \frac{2hc^2}{\lambda^5} \frac{1}{e^{(hc/\lambda kT)} - 1}$$

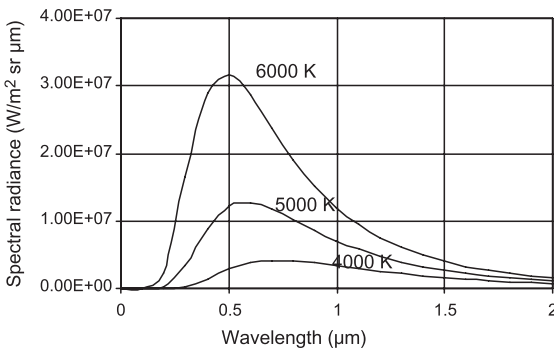
$h = 6.626 \times 10^{-34} \text{ J} \cdot \text{s}$
 (Planck's constant)
 $c = 2.998 \times 10^8 \text{ m} \cdot \text{s}^{-1}$
 $k = 1.381 \times 10^{-23} \text{ J} \cdot \text{K}^{-1}$
 (Boltzmann's constant)

More commonly, Planck's Law is stated as:

$$L_{\lambda} = \frac{c_1}{\pi n^2 \lambda^5} \frac{1}{e^{c_2/n\lambda T} - 1}$$

$c_1 = 2\pi h c^2 = 3.742 \times 10^{-16} \text{ W} \cdot \text{m}^2$
 (first radiation constant)
 $c_2 = hc/k = 1.439 \times 10^{-2} \text{ m} \cdot \text{K}$
 (second radiation constant)

The units of the above equation are $\text{W}/\text{m}^2 \text{sr m}$. Results are often desired per nanometer or per micrometer, and care must be used when converting from one unit to another.



Blackbody radiation occurs when the emittance of the radiating material over all wavelengths is 1, as in the above figure showing blackbody radiation for several temperatures. When the emittance is constant but nonunity, the material is said to radiate as a **graybody**. When the emittance is a function of wavelength, i.e., $\varepsilon = \varepsilon(\lambda)$, the material is called a **selective radiator**. Although there are no perfect blackbodies in nature, the model is a good one for many sources, including the sun.

Stefan–Boltzmann and Wien Displacement Laws

The **Stefan–Boltzmann law** provides the total radiant exitance from a blackbody source over all wavelengths:

$$M = \sigma T^4$$

σ = Stefan–Boltzmann constant, $5.67 \times 10^{-8} \text{ W/m}^2 \text{ K}^4$

T = temperature, in kelvin.

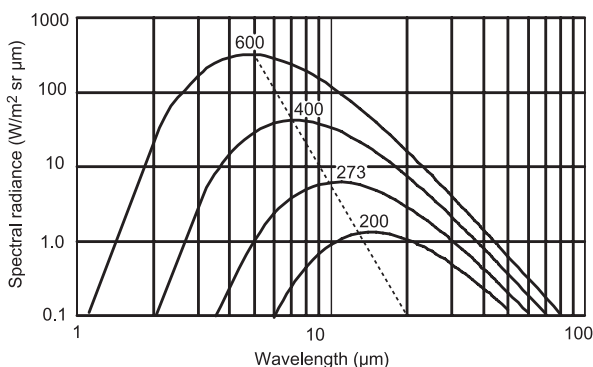
The radiant exitance of a greybody is its emittance ε , multiplied by this result. The radiance of a blackbody may be obtained from total radiant exitance by dividing by π :

$$L = \frac{M}{\pi}$$

The **Wien displacement law** (often referred to as **Wien's law**) provides the wavelength, in micrometers, of maximum spectral radiance (or radiant exitance) of a blackbody given its temperature in kelvin:

$$\lambda_{max} T = 2898 \text{ } \mu\text{m} \cdot \text{K}$$

When blackbody spectral radiance (or radiant exitance) is plotted against wavelength for several temperatures on a log–log scale, Wien's law is graphically represented by a straight line drawn through the curve peaks.



Rayleigh–Jeans Law and Wien Approximation

Two common approximations to the Planck equation are applicable in certain circumstances. The **Rayleigh–Jeans law**, for long wavelengths and/or high temperatures, is:

$$L_{\lambda} = \frac{2ckT}{\lambda^4}$$

c = speed of light
 k = Boltzmann's constant
 T = temperature in kelvin

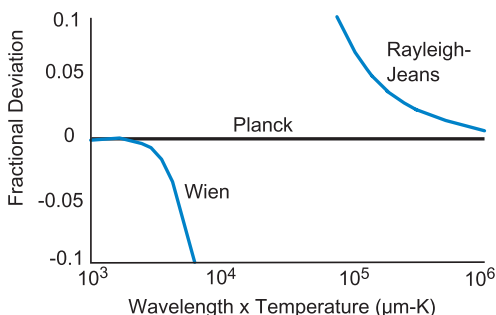
Note that Planck's constant does not appear in the law because it applies to wavelengths longer than those for which quantum effects must be considered. The Rayleigh–Jeans law is valid with less than 1% error if $\lambda T > 0.778 \text{ m} \cdot \text{K}$. The approximation is not used frequently, as less than 0.1% of blackbody output occurs at λT values greater than $0.8 \text{ m} \cdot \text{K}$.

Of more utility is the **Wien approximation**, valid for short wavelengths and/or low temperatures:

$$L_{\lambda} = \frac{c_1}{\pi\lambda^5} e^{-\frac{c_2}{\lambda T}}$$

c_1 and c_2 are the first and second radiation constants, respectively.

The Wien approximation is valid with less than 1% error if $\lambda T < 3000 \text{ } \mu\text{m} \cdot \text{K}$, and is widely applicable.

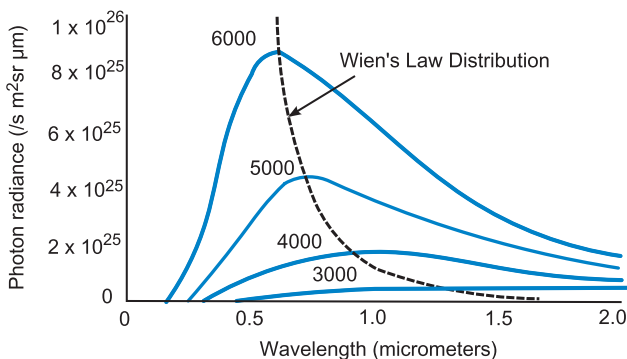


The Rayleigh–Jeans law was dubbed the “ultraviolet catastrophe” by physicist Paul Ehrenfest due to its projection of infinite radiance at $\lambda = 0$.

Radiation Laws in Terms of Photons

As was the case for quantities expressed in terms of watts, all radiation laws have analogous expressions in terms of photons per second. In the case of vacuum ($n = 1$; therefore $\lambda = \lambda_0$):

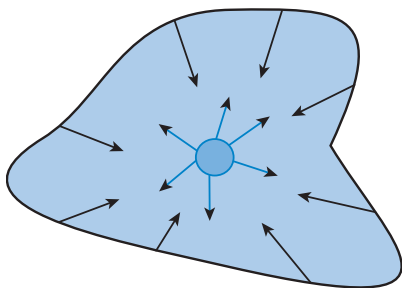
$L_{q\lambda} = \frac{c_{1q}}{\pi\lambda^4} \frac{1}{e^{c_2/\lambda T} - 1}$	Photon spectral radiance; $c_{1q} = 2\pi c = 1.883 \times 10^9 \text{ m/s}$; $L_{q\lambda}$ is in photons/ s m ² sr m
$\lambda_{q,\max} T = 3700 \text{ } \mu\text{m} \cdot \text{K}$	Wien displacement law for photons
$L_{q\lambda\max} = \frac{\sigma'_q}{\pi} T^4$	Photon spectral radiance at the peak; $\sigma'_q = 2.1 \times 10^{11} \text{ s}^{-1} \text{ m}^{-2} \text{ K}^{-4} \text{ } \mu\text{m}^{-1}$
$L_q = \frac{\sigma_q}{\pi} T^3$	Total photon radiance (Stefan–Boltzmann law); $\sigma_q = 1.52 \times 10^{15} \text{ s}^{-1} \text{ m}^{-2} \text{ K}^{-3}$



The locus through the peaks of the curves represents Wien's displacement law.

In some cases, it is desirable to use photon spectral radiance rather than its power-related sister distribution. For example, problems for which photon detection is required make good candidates for photon radiance distribution usage.

Kirchoff's Law



A small blackbody enclosed in an isothermal ($\Delta T = 0$) cavity will have the same temperature as its enclosure when the system is at thermal equilibrium. Absent additional radiation sources or sinks, the power emitted by

the source must equal the power it absorbs: $\alpha\Phi_i = \varepsilon\Phi_{BB}$. Because the incident and emitted power are the same,

$$\alpha = \varepsilon,$$

which is **Kirchoff's law**. However, in addition to thermal equilibrium, spectral and directional constraints must also be applied to the above expression.

Directional Spectral $\alpha(\lambda; \theta, \phi, T) = \varepsilon(\lambda; \theta, \phi, T)$

No constraints other than thermal equilibrium

Directional Total $\alpha(\theta, \phi, T) = \varepsilon(\theta, \phi, T)$

- (1) Spectral distribution of incident power proportional to BB at T , or
- (2) α and ε independent of wavelength

Hemispherical Spectral $\alpha(\lambda, T) = \varepsilon(\lambda, T)$

- (1) Incident power independent of angle, or
- (2) α and ε independent of angle

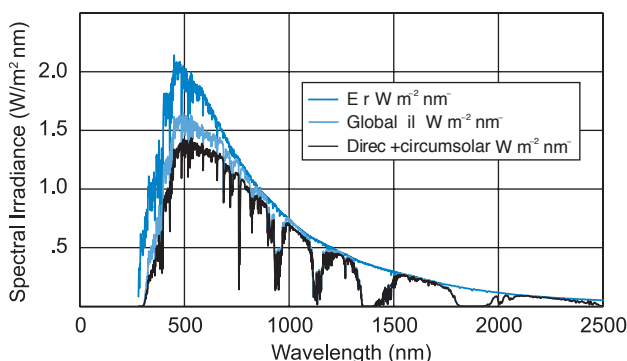
Hemispherical Total $\alpha(T) = \varepsilon(T)$

- (1) Incident power independent of angle and spectral distribution proportional to BB at T ; or
- (2) Incident power independent of angle and α , ε independent of wavelength; or
- (3) Incident power at each angle has spectral distribution proportional to BB at T and α , ε independent of angle; or
- (4) α and ε independent of both angle and wavelength

(Table derived from Ref. 2)

Natural Sources

Sources of radiation may be classified in a variety of ways, including natural or artificial. Among **natural sources** are the sun, moon, the earth, zodiacal radiation, and even humans. Each of these sources may be further classified as **active** or **passive**, depending on whether they generate radiation, as the sun does, or reflect it, like the moon. Some sources are both active and passive: zodiacal light results from solar reflection off dust in the visible spectrum; in the infrared, the radiation mechanism is thermal emission from dust particles.



The sun is our primary source of natural radiation on earth. For applications such as solar photovoltaics, direct solar illumination and global illumination (from a hemisphere) are often considered.

The above plot utilizes a portion of the **ASTM G-173-03 reference spectrum** for an **airmass** of 1.5. Airmass is defined as the secant of the solar zenith angle, with an airmass of 1 indicating that the sun is directly overhead. Airmass 1.5 implies a solar zenith angle of about 48 deg or an elevation angle of about 42 deg.

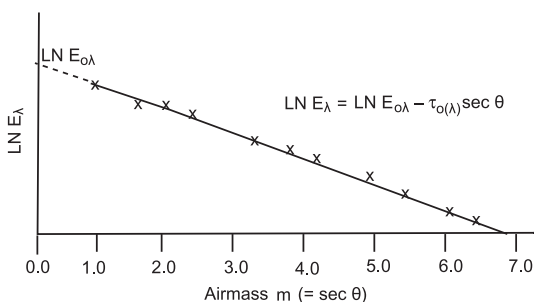
The earth (300 K) becomes a primary source of radiation in the IR, particularly in the atmospheric window 8–12 μm .

Lambert–Bouguer–Beer Law and Langley Plot

The **Lambert–Bouguer–Beer law** describes attenuation not only within optical media but also within the atmosphere as well. In this application it expresses the wavelength-dependent irradiance received at a point on earth as a function of the exoatmospheric spectral irradiance:

$$E_{\lambda} = E_{o\lambda} e^{-\tau_{o(\lambda)} m}$$

where $E_{o\lambda}$ = exoatmospheric spectral solar (or stellar) irradiance, m = airmass, and $\tau_{o(\lambda)}$ = atmosphere's optical thickness at that wavelength.



The law is strictly valid only monochromatically and assumes an unchanging atmosphere during the measurement period. Note that $E_{\lambda}/E_{o\lambda}$ is also called **transmittance**.

This information can be transferred to a **Langley plot**, which expresses irradiance at one wavelength as a function of airmass. The slope of the line is the **spectral optical thickness** $\tau_o(\lambda)$; the y intercept is the exoatmospheric solar irradiance at that wavelength that may be obtained by extrapolation. $\tau_o(\lambda)$ is also called **optical depth**:

$$\tau_o(\lambda) = e^{-\alpha'(\lambda)x}$$

The absorption coefficient may be further divided into molecular and aerosol scattering, and absorption components.

Artificial Sources

Natural and **artificial sources** may be classified as either **thermal** or **luminescent**. Thermal sources emit radiation as a function of temperature or reflect it; luminescent sources emit radiation via atomic transitions. Some sources are both thermal and luminescent. Artificial sources vary widely in type and spectral characteristics; measurements must always take into account spectral, directional (geometric), and spatial properties of the radiation.

Thermal sources

Incandescent lamps
Hot metals
Exhaust gases
(CO₂, CO, H₂O)
Electrical wiring
Globar, carbon arc
Soot
Optical elements
Paint
Glass

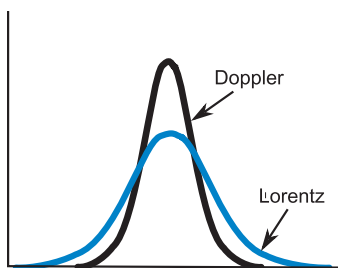
Luminescent sources

LEDs, IREDs, OLEDs
Phosphors
Exhaust gases
(CO₂, CO, H₂O)
Fluorescent lamps, CFLs
Lasers
Laser diodes
Sodium vapor lamp
Mercury vapor lamp
Xenon arc

Exhaust gases, such as from diesel engines or muzzle flash, emit radiation at wavelengths where they are optically thick and often include the blackbody contribution of particulates >30 μm in diameter.

If a gas spectrally absorbs where it emits, how can we see it? Due to higher temperature and pressure, a hot gas will have a slightly different spectral profile than an unheated one. While the center wavelength will absorb, the hot gas may be observed in the two wavelength regions bordering the center, as a function of temperature, pressure, spectral region, and emitting species.

Luminescent Mechanisms



Although temperatures must be high to achieve significant radiation from thermal sources in the visible and UV (the sun, for example, is often modeled as a 6000 K blackbody), luminescence generates radiation at lower temperatures. Doppler

(Gaussian) and pressure (Lorentzian) effects provide broadening of spectral lines, so that emission is not strictly “monochromatic,” but it exists in a narrow spectral region. Luminescent sources tend to be more efficient than thermal sources in generating light, as their spectra can be engineered to fall in the visible band with little or no infrared.

Doppler Effects

Low-pressure discharge
 Little power in each line
 Sharp line applications
 Wavelength calibration
 –Fluorescence excitation
 –Interferometry

Low-pressure lamps
 –Hg, He, Ne, Na, K,
 Zn,Cd, Cs

Lorentzian Effects

Pressure-broadened lines
 High radiant power, efficient
 Wings combine to form
 continuum
 –Illumination, searchlights
 –Projection systems
 –Solar simulators
 High-pressure lamps
 –Hg, Xe, Hg-Xe, Na
 –Can be modulated and
 flashed

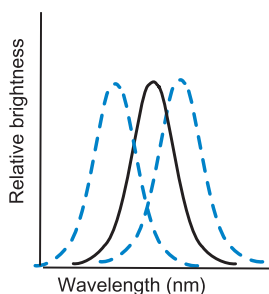
A low-to-moderate-pressure mercury discharge source (254-nm line) becomes a **fluorescent source** with the addition of a phosphor, allowing the UV photons absorbed by the phosphor to cause emission of visible photons we see as light. **Compact fluorescent lamps (CFLs)** are higher-efficiency variants packed into a smaller volume. They are increasingly used in many household applications in place of **incandescent** (tungsten-filament) lightbulbs.

Some Luminescent Sources

Light-emitting diodes (LEDs)

utilize a forward-biased p - n junction to generate radiation. The emission comes from recombination radiation at the band edge excited by high current density. The emission spectral region is narrow, about 5% of the center wavelength. LEDs are small, consume little power, and have lifetimes greater than 10,000 hrs. They are finding increasing use in lighting applications, replacing incandescent sources in traffic and roadway lighting, automobiles, and airline cockpits. They are available in a variety of wavelengths.

Red, green, and blue LEDs may be combined to produce a “white” LED. White LEDs may also be produced by using a blue LED in conjunction with a specific phosphor (such as Cs:YAG) to produce radiation over a broader region from about 500 to 700 nm.



Material	λ (nm)
GaN	350
SiC	465
GaP	565
ZnTe	620
CdTe	855
InP	1000
ZnCdTe	530–830
AlGaAs	620–900
InGaAs	850–3150

Organic light-emitting diodes (OLEDs), a class of LED made from polymers and other organic materials, have very thin width and are competing with LCDs as “sheet displays” in many applications.

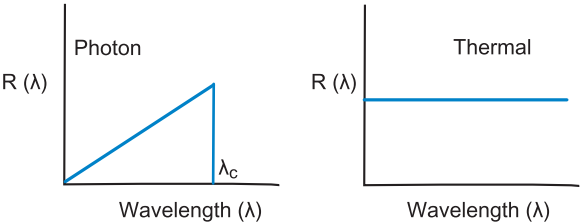
Lasers (an acronym for Light Amplification by Stimulated Emission of Radiation) operate due to photon stimulation or induction of an excited-state molecule to induce a secondary photon emission, in phase with the initial photon. As a result, lasers are coherent sources, and the power transfer laws detailed herein generally do not apply unless the laser is coupled to an integrating sphere to produce a diffuse beam.

Detector Types

Detectors of optical radiation may be classified several different ways: there are **point** and **area** detectors, **thermal** and **photon** detectors, and various kinds of arrays. The **responsivity** \mathfrak{R} (A/W or V/W) of a photon or thermal detector is the ratio of output electrical signal to incoming radiant power:

$$\mathfrak{R} = \frac{\int R(\lambda)\Phi_{\lambda}d\lambda}{\int \Phi_{\lambda}d\lambda}$$

Both power and responsivity may be expressed as spectral or total quantities. Ideal responsivities are shown below.



Photon responsivity \mathfrak{R}_q is defined analogously, with the input being photon flux (photons/s) and the output a current or voltage.

The **cutoff wavelength** λ_c is the wavelength at which a detector ceases to be responsive.

There are several significant differences between photon and thermal detector categories in addition to the shape of their response curves.

Parameter	Thermal	Photon
Spectral response	Wide	Narrow
Detectivity	Low	High
Response time	Slow	Fast
Cooling	Not typical	Typical in IR
Chopping	Often	Rarely
Cost (IR)	Low	High

Detector Definitions

Cutoff frequency f_c is the electrical frequency, in Hz, at which the detector response falls to 0.707 of its midband maximum value. It is also called **3-dB frequency**.

Time constant τ is the time required for a signal to achieve 63% of its final output, given a step input:

$$\tau = \frac{1}{2\pi f_c}$$

Thermal time constant τ_T is defined analogously to electrical time constant, $1/(2\pi f_T)$. It characterizes a thermal detector's speed of response, with f_T called the **thermal cutoff frequency**.

rms (root-mean-square) value (voltage or current) is defined mathematically as

$$v_{rms} = \sqrt{\frac{1}{T} \int_0^T v^2(t) dt}$$

where T is a single or integer multiple period, for a periodic waveform.

Responsive quantum efficiency η is the number of independent output events per incident photon, often expressed in electrons/photon. It is also called **quantum efficiency**.

Curie temperature T_c is the temperature at which a ferroelectric material loses its polarization. It is important in pyroelectric detectors.

It is always important to note the units of responsivity \mathfrak{R} , particularly since the same term is used to describe the radiometric performance of an entire system. In the latter cases, **irradiance responsivity** \mathfrak{R}_E and **radiance responsivity** \mathfrak{R}_L are commonly seen.

More Detector Definitions

Signal v_s or i_s is the rms component of detector output voltage or current arising from a specific radiometric input.

Noise v_n or i_n is the rms component of detector output voltage or current arising from random fluctuations in the detector circuit, incoming radiation, and other factors.

Signal-to-noise (SNR) ratio (in amplitude) may be defined in terms of either voltage or current. It is dimensionless.

$$SNR = \frac{v_s}{v_n} = \frac{i_s}{i_n}$$

Impedance Z (ohms) is the slope of the current versus voltage curve of a device at the designated operating point.

$$Z = \frac{dV}{dI}$$

RA product is the product of a detector resistance and its area and is a constant for many materials.

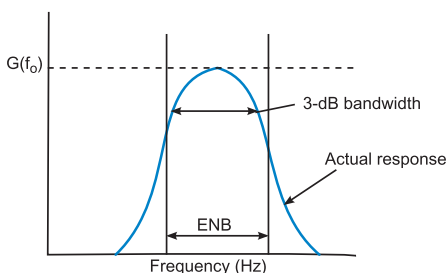
BLIP is an acronym for Background-Limited Infrared Photodetector, one for which the limiting noise in the detector output arises from background (not signal) photons.

Effective noise bandwidth B (also ENB and Δf) is an equivalent square-band bandwidth, differing from the 3-dB bandwidth.

$$B = \frac{1}{G(f_o)} \int_0^\infty G(f) df$$

For spectrally flat (white) noise, G = power gain f_o = frequency where G is maximum.

Advantage of ENB: total noise power can be obtained by multiplying ENB by the power spectral density, as long as the latter is constant.



Detector Figures of Merit

Detective quantum

efficiency DQE is the ratio of the squares of output and input SNR .

$$DQE = \frac{SNR_{out}^2}{SNR_{in}^2}$$

Noise equivalent

power NEP (W) is the input power producing a unity SNR .

$$NEP = \frac{v_n}{\Re} = \Phi \frac{v_n}{v_s}$$

Detectivity D (W^{-1}) is the reciprocal of the NEP .

$$D = \frac{1}{NEP} = \frac{SNR}{\Phi_{input}}$$

Specific detectivity D^*

($cmHz^{1/2}W^{-1}$) is D normalized for detector area and noise bandwidth B .

$$\begin{aligned} D^* &= D \sqrt{A_d B} = \frac{\sqrt{A_d B}}{NEP} \\ &= \frac{\sqrt{A_d B}}{\Phi} \frac{v_s}{v_n} \end{aligned}$$

D^{**} ($cmHz^{1/2}W^{-1}$) normalizes D^* to a π sr projected solid angle FOV. It is pronounced, "Dee double-star."

$$D^{**} = D^* \sqrt{\frac{\Omega}{\pi}} = D^* \sin \theta_{1/2}$$

All **figures of merit** have both spectral and photon formulations, e.g., $D^*(\lambda)$ is D^* at a specific wavelength:

$$D^*(\lambda) = \frac{\sqrt{A_d B}}{NEP(\lambda)} \text{ cm} \cdot \text{Hz}^{1/2}/\text{W}$$

Photon D^* is the specific or normalized detectivity in terms of photons:

$$D^*_q = D^* \frac{hc}{\lambda} = \frac{\sqrt{A_d B}}{\bar{n}} \frac{i_s}{i_n} \text{ cm} \cdot \text{Hz}^{1/2}/(\text{photons/s})$$

where \bar{n} in the denominator is the photon flux in photons per second at wavelength λ .

Noise Concepts and Definitions

Noise can be expressed as a voltage, current, or power, and is best expressed as a spectral (per Hz) quantity if its magnitude depends on frequency. The **mean-square noise voltage** (equivalent to **noise power**) is:

$$\overline{v^2} = \overline{(v_i - v_{avg})^2} = \frac{1}{T} \int_0^T (v_i - v_{avg})^2 dt$$

where v_i = instantaneous voltage, v_{avg} = average voltage, and T = observation time.

Current may be used with the substitution (**Ohm's law**):

$$\overline{i^2} = \frac{\overline{v^2}}{R^2}$$

Independent (uncorrelated) noise powers add algebraically; noise voltages or currents add in quadrature.

$$v_n^2 = v_1^2 + v_2^2 + \cdots + v_i^2$$

$$v_n = \sqrt{\overline{v_1^2} + \overline{v_2^2} + \cdots + \overline{v_i^2}}$$

Noise factor F is the ratio of a detector's actual noise to the theoretical limit.

$$F = \frac{\text{real noise power}}{\text{ideal noise power}} = \frac{SNR_{in}}{SNR_{out}} = \frac{1}{\sqrt{DQE}}$$

Noise figure NF is the \log_{10} of the noise factor. Expressed in dB, it is

$$NF = 10 \times \log \left[\frac{\text{real noise power}}{\text{ideal noise power}} \right] \text{ dB}$$

Noise temperature T_n is the temperature of a thermal source providing a signal power equal to the noise power.

$$T_n = \frac{v_n^2 + i_n^2 R^2}{4kRB}$$

The Most Unpleasant Noises

Johnson noise (Nyquist, thermal) occurs due to random motion of carriers in any electrical conductor. The second expression is valid when B is established by an RC circuit time constant.

$$v_j = \sqrt{4kTRB}; \quad v_j = \sqrt{kT/C}$$

k = Boltzmann's constant
 1.38×10^{-23} J/K
 T = Temp (K)
 R = resistance, Ω
 C = capacitance, F

Shot noise occurs due to the discrete nature of electronic charge (as in vacuum tubes, for example) seen when current flows across a potential barrier.

$$i_s = \sqrt{2qI_{dc}B}$$

q = elec. charge,
 1.6×10^{-19} C
 I_{dc} = direct current across a potential barrier

Generation-Recombination (G-R) noise arises from fluctuations in the rate at which charge carriers are generated and recombined within semiconductors. The equation form depends on detector configuration. G-R is not present in thermal detectors.

$$v_{G-R} = 2\bar{i}R \sqrt{\frac{\tau_l B}{N[1 + (2\pi f \tau_l)^2]}}$$

(extrinsic photoconductor)
 N = mean number of carriers
 \bar{i} = average photocurrent due to N
 τ_l = carrier lifetime

1/f noise is insidious noise from various sources. It is ubiquitous and does not decrease through integrating over time.

$$i_{1/f} = \sqrt{\frac{K_s I_{dc}^\alpha B}{f^\beta}}$$

$1.25 < \alpha < 4$ (typically 2)
 $0.8 < \beta < 3$ (typically 1)
 K_s is source dependent

Temperature fluctuation noise occurs due to microfluctuations in thermal detector temperature. It is related to the statistical noise in blackbody radiators.

$$\Delta T = \sqrt{\frac{4kT^2KB}{K^2 + 4\pi^2 f^2 H^2}}$$

K = thermal conductance (W/deg)
 H = heat capacity (J/deg)

More Unpleasant Noises

Photon noise arises because photons randomly arrive at the detector. Photons obey Poisson statistics, so the mean-square fluctuations in the photon arrival rate are equal to the arrival rate, with n the number of photons.

$$\sqrt{(\Delta n)^2} = \sqrt{n}$$

Microphonic noise is acoustically generated. It is found in pyroelectric thermal detectors, which act like microphones. Unanchored wiring in a vacuum dewar also produces this noise.

Triboelectric noise originates from charges built up within dielectrics, typically within coaxial cables.

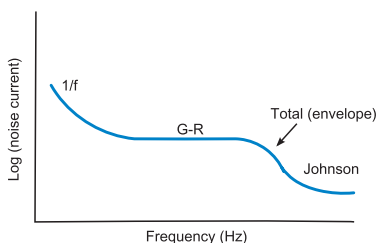
Amplifier noise is a form of $1/f$ noise typically found in low-level circuitry coupled to the detector output. It is usually related to f^2 .

Quantization noise occurs when analog signals are digitized. It is related to the number of bits n in the digital word, with LSB the magnitude of the least significant bit and $SIGNAL_{max}$ the full-scale signal.

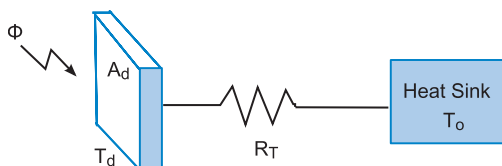
$$LSB = \frac{SIGNAL_{max}}{2^n}$$

CCD noises arise from processes related to charge transfer and readout in CCD arrays, including variations in **charge transfer efficiency (CTE)**, readout noise, and **kT/C noise** arising from the residual charge left on an integrating capacitor after a reset switch is closed and opened.

For a photoconductive detector, $1/f$, G-R, and Johnson noise voltages are uncorrelated (independent) and add in quadrature.



Thermal Detectors



In **thermal detection**, incident radiation is absorbed by the detector's receiving surface, causing an increase in surface temperature. The temperature change is detected by one of several means, giving rise to thermoelectric detectors, resistive bolometers, pyroelectric detectors, and others. All thermal detectors operate according to the same relationship between incident radiation, the detector, and its immediate surroundings:

$$\Delta T = T_d - T_o = \frac{\alpha \Phi R_T}{\sqrt{1 + \omega^2 R_T^2 H^2}} \quad \begin{array}{l} T_d = \text{detector temp} \\ T_o = \text{heat sink temp} \end{array}$$

R_T = thermal resistance between receiver and heat sink (deg/W)

H = heat capacity of receiver (J/deg)

ω = radian frequency of incoming signal

α = detector material absorptance

Φ = incident radiant power $\Phi_0 e^{j\omega t}$ to allow for either steady-state or modulated (chopped) radiation.

Thermal time constant

$$\tau_T = R_T H$$

Thermal resistance

σ = Stefan–Boltzmann constant

$$R_T = \frac{1}{4\alpha\sigma A_d T_d^3}$$

Thermal conductance

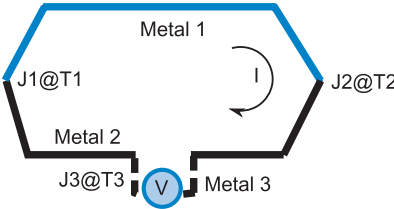
$$K = \frac{1}{R_T}$$

In the theoretical limit, noise occurs due to fluctuation in input signal power (analogous to photon noise, for photon detectors). In practice, this limit is rarely achieved, and the detector is typically Johnson-noise limited.

$$NEP = 4\sqrt{\frac{kT_d^5 \sigma A_d B}{\alpha}}$$

Thermoelectric Detectors

Thermoelectric detectors operate according to the **thermoelectric effect**, in which a temperature difference produces a voltage difference (and vice versa). Given two dissimilar metals connected in series (a thermocouple) and placed in a circuit, a current will flow in the direction indicated



if temperature T_2 in metal 2 is greater than T_1 in metal 1. Opening the circuit to check the voltage due to current flow yields S , the **Seebeck coefficient** or thermoelectric power.

$$S = \frac{\Delta V}{\Delta T} \text{ (V/deg)}$$

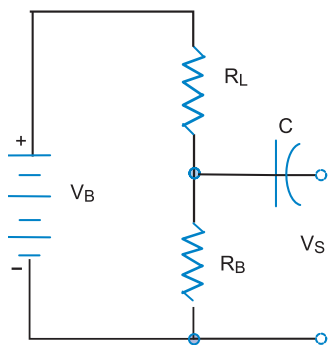
$\Pi = \frac{1}{I} \left(\frac{dQ}{dt} \right)$ The **Peltier effect** occurs when current is passed through a thermoelectric circuit, resulting in one of the junctions between the two materials becoming warm while the other cools. The **Peltier coefficient** Π describes the effect's magnitude in terms of heat flow (dQ/dt) and current I . This effect is exploited in thermoelectric coolers used to cool detectors, laser diodes, dew-point sensors, and other devices.

The Peltier effect also causes a reduction in sensitivity (reduced ΔT). The signal, however, may be increased by placing several junction pairs in series to form a **thermopile**. Johnson noise predominates.

$$\Delta T = \alpha \Phi R_T \left(1 - \frac{R_T S^2 T_d}{R} \right)$$

Material	$S \text{ (}\mu\text{V/}^\circ\text{C)}$	Material	$S \text{ (}\mu\text{V/}^\circ\text{C)}$
Al	−0.5	Bi	−60
Cu	+2.7	Sb	+40
Ag	+2.9	Fe	+16

The Bolometer



A thermoresistive material that absorbs radiation becomes warmer, and the resulting change in its electrical resistance can be sensed using a **bolometer**, a resistor possessing a high **temperature coefficient of resistance (TCR)**. TCR is denoted by β and is in units of K^{-1} . Bolometers may be fabricated

from metals (classical) or semiconductors (more recent).

To measure resistance, a current must be forced through the circuit; the half-bridge configuration is common for this device, with the coupling capacitor used for blocking the DC signal across the sensitive component R_B .

Signal voltage measured across the terminals is

$$V_s = \Delta V = \frac{V_B R_L \Delta R_B}{(R_B + R_L)^2}$$

If $R_L = R_B$ (maximum power transfer theorem),

$$V_S = \Delta V = \frac{V_B R \Delta R}{(R + R)^2} = \left(\frac{V_B}{4} \right) \left(\frac{\Delta R}{R} \right) = \left(\frac{V_B}{4} \right) \left(\frac{R_o \beta \Delta T}{R} \right)$$

The bolometer voltage responsivity is then:

$$\mathfrak{R}_v = \frac{V_s}{\Phi} = \left(\frac{V_B}{4} \right) \left(\frac{\alpha \beta R_T}{\sqrt{1 + \omega^2 \tau_T^2}} \right)$$

Relatively low-cost infrared cameras using uncooled semiconductor microbolometer arrays have become increasingly popular in recent years. It is not uncommon in today's (2011) market to see cameras with less than 20- μm pixel size in a 640 \times 480 array.

Pyroelectric Detectors

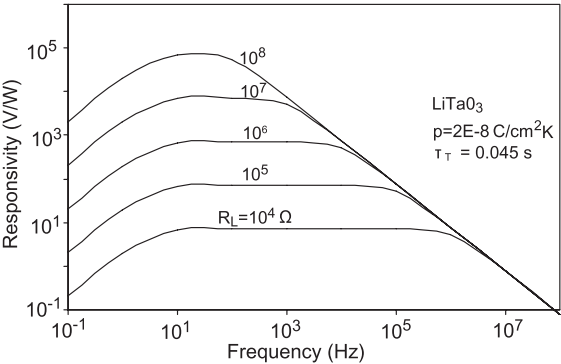
The **pyroelectric effect** displayed in some ferroelectric materials is a change in surface charge with temperature. This property is used in the pyroelectric detector, which is capable of high-speed operation and responds only to changes in the input signal (which requires chopping). The **pyroelectric coefficient** p is the change in electric polarization due to a change in temperature:

$$p = \frac{dP_s}{dT} \text{ C/cm}^2\text{K}$$

p increases until the material's Curie temperature is reached, above which it drops to zero.

$$\mathfrak{R}_v = \frac{\alpha \omega p A_d R_L R_T}{\sqrt{1 + \omega^2 \tau^2} \sqrt{1 + \omega^2 \tau_T^2}}$$

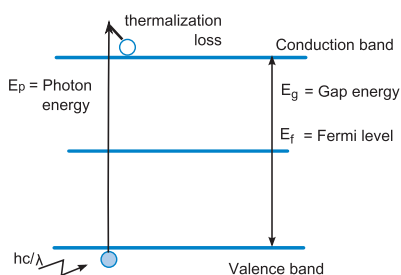
The voltage responsivity of pyroelectric detectors is a function of both thermal and electrical frequencies, the pyroelectric coefficient, thermal resistance, and load. There is the typical speed–sensitivity tradeoff issue.



Material	p (C/cm ² K)	D^* (cmHz ^{1/2} /W)	Remarks
TGS	4×10^{-8}	10^9	High D^*
LiTaO ₃	2×10^{-8}	6×10^8	“Bulletproof” ¹
SrBaNbO ₃	6×10^{-8}	5×10^8	Fastest
PVF ₂	2×10^{-8}	2×10^8	Cheap

¹ James M. Palmer (1937–2007)

Photon Detectors



Photon detection relies on materials that allow an incident photon with sufficient energy to elevate an electron from a bound state (**valence band**) to a free state (**conduction band**) where, depending

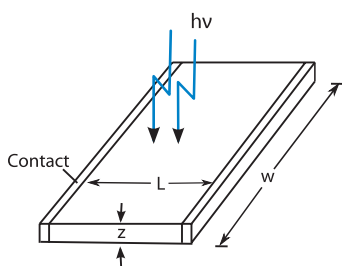
on the detection mechanism, it is available for conduction under an applied electric field or (in the photoemissive case) for escape into vacuum.

The energy of the incident photon must be greater than or equal to the **gap energy** E_g , and the **cutoff wavelength** (μm) for this process may be expressed as $\lambda_c = 1.24/E_g$ with energy in eV. The difference between E_p and E_g constitutes **thermalization loss** and causes the voltage and power in a solar photovoltaic cell to decrease. E_f is the **Fermi level**, which has a 50% probability of being occupied by an electron.

Materials useful in photon detection include **intrinsic semiconductors** having only a small concentration of impurities and **extrinsic semiconductors** into which impurities have been introduced via the doping process to extend the wavelength response.

Material	Energy gap (eV)	λ_c (μm)
SiC	3.0	0.41
CdS	2.4	0.52
GaP	2.25	0.55
Si	1.12	1.1
Ge	0.68	1.8
PbSe	0.26	4.8
$\text{Hg}_{(1-x)}\text{Cd}_x\text{Te}$	variable	1 to 24

Photoconductive Detectors



The **conductivity** σ_e of a slab of semiconductor material is a function of electron concentration, hole concentration (the positions left in the valence band after an electron moves into the conduction band), electronic charge q , and mobility of

electrons and holes. When the detector based on this material is placed into a circuit and bias voltage applied, a voltage responsivity can be computed:

$$\mathfrak{R}_v = \frac{I_{dc} R \lambda \eta q \mu \tau_l}{2 h c z A_d \sigma_e}$$

where η = quantum efficiency, μ = carrier mobility (generally the sum of electron and hole mobilities), τ_l = carrier lifetime, and σ_e = electrical conductivity ($\Omega \cdot \text{cm}$)⁻¹.

The **photoconductive gain** G of the device is the ratio of the carrier lifetime to the carrier **transit time** τ_{tr} between the electrodes.

$$G = \frac{\tau_l}{\tau_{tr}}$$

Noise current in photoconductive detectors is:

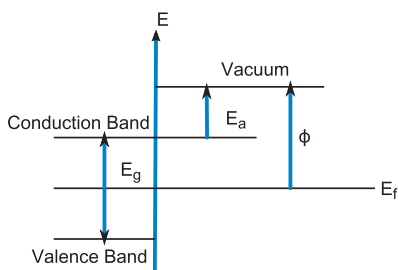
$$\overline{i_n^2} = 4q \left[\eta q \Phi \left(\frac{\lambda}{hc} \right) G^2 + q G^2 N' + \frac{kT}{qR_D} + \frac{kT}{qR_L} \right] B$$

Terms inside the bracket, according to order:

1. G-R noise from incident photons (signal and background)
2. Dark current noise due to N' thermally generated carriers
3. Johnson noise in the detector resistor, R_D and
4. Johnson noise in the load resistor R_L

$D^{*BLIP}(\lambda, f) = \lambda / 2hc \times (\eta / E_q)^{1/2}$, where E_q is photon incidence.

Photoemissive Detectors



The process of photoemission relies on an **external photoeffect**, in which an electron receives sufficient energy from an incident photon to physically escape a photosensitive material called a **photocathode**.

In this three-step process, a photon is absorbed, resulting in a “hot” electron; the electron moves to the vacuum interface; and the electron escapes over the surface barrier into the vacuum, where, in practical devices, it is captured by a positively charged anode.

The **work function** ϕ is the energy required for an electron to escape the surface barrier. For both metals and semiconductors, it is used to calculate the **cutoff wavelength** according to $\lambda_c = 1.24/\phi$ with λ in micrometers and ϕ in eV.

An expression for noise voltage is:

$$v_n = R_L \left[\left(2qi_d + 2q^2\eta\Phi \frac{\lambda}{hc} + \frac{4kT}{R_L} \right) B \right]^{1/2}$$

Terms inside the bracket:

1. Shot noise due to dark current i_d
2. Shot noise due to signal + background current
3. Johnson noise in load resistor R_L

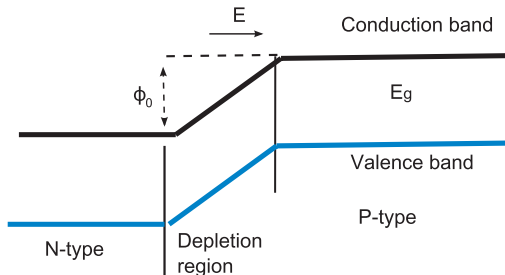
Johnson noise and dark current are reduced by cooling, leaving signal-dependent shot noise as the main noise source.

Current responsivity for a photocathode: $\mathfrak{R}_i = q\eta\lambda/hc$

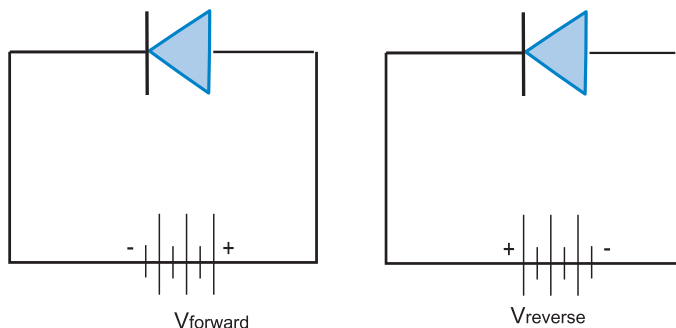
Prominent photoemissive detectors are the **photomultiplier tube (PMT)** and microchannel plates.

Photovoltaic Detectors

The **photovoltaic detector** responds to incoming photons striking a ***p-n junction*** in a semiconductor material. The junction is formed by doping adjacent areas differently so that one becomes an ***n-type*** (donor) and the other a ***p-type*** (acceptor) of electrons. The physical area between these two sections is called the **depletion region**, which contains an electric field due to ionized donors and acceptors. That electric field creates a **potential difference** ϕ_0 between *p* and *n* regions, shifting the band energies of the two materials.



If a forward bias is applied to the *p* region, the potential barrier height is reduced, current flow increases, and the depletion region narrows. If a reverse bias is applied to the *n* region, the barrier height is increased, the current decreases, and the depletion region widens.

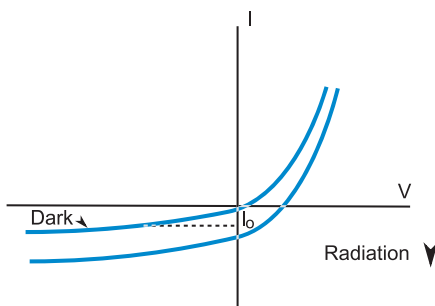


Photovoltaic devices are often used as power generators, as in the case of a solar cell.

Photovoltaic Current and Performance

In the absence of optical radiation on the photodiode, there is no photocurrent through the detector, and the detector's dark level is defined by the **reverse saturation current** I_0 .

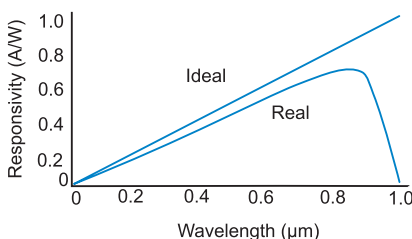
Incident optical radiation generates a current through the diode, shifting the current-voltage (I-V) curve downward. The expression for total current through the diode becomes



$$I = I_0 \left(e^{\frac{qV}{\beta kT}} - 1 \right) - I_g$$

with I_g = photocurrent, β = “ideality factor” that varies with applied voltage—1 for the ideal case, but 2–3 for the real case. The current responsivity of photovoltaic detectors is $\mathfrak{R}_i = \eta q \lambda / hc$.

The detector is shot-noise dominated. Noise current may be expressed as a function of the



signal current in the visible spectrum: $i_{shot} = (2q i_s B)^{1/2}$. In the infrared, shot noise current is a function of the background:

$$i_{shot} = \left[2\eta q^2 \lambda / hc \Phi B \right]^{1/2}$$

Johnson noise in the load resistor and $1/f$ noise are also present but play less significant roles.

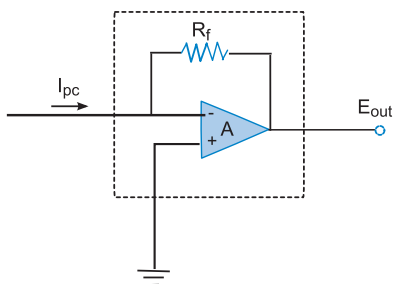
$$D_{BLIP}^*(\lambda, f) = \eta \lambda / (2E_{back} hc)^{1/2}$$

where E_{back} is the background irradiance.

Detector Interfacing

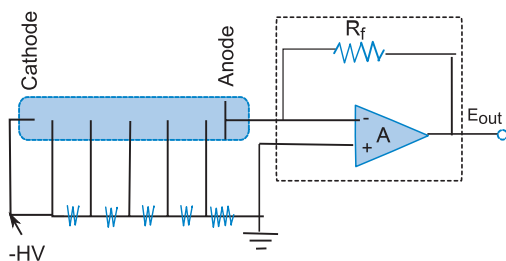
A detector of optical radiation functions as a transducer, converting one form of energy to another to produce an output electrical signal. Amplifiers operate on the output signal to bring it up to a level compatible with the circuitry used in the electrical subsystem.

Calculations of the SNR out of an amplifier must take into account the value of the feedback resistor (if applicable) and various noise sources, which may include Johnson noise, shot noise, and $1/f$ noise, along with noise in the amplifier itself.



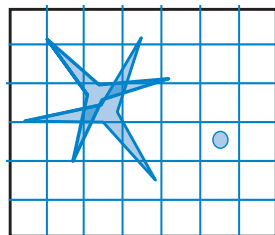
$SNR = \text{signal voltage out} / \text{noise voltage out}$. In this case, where the pre-amp may be coupled to the output of a photovoltaic device, $E_{out} = -I_{pc}R_f$, where I_{pc} is the photocurrent from the detector and R_f is the value of the feedback resistor.

More than one detector type may utilize a particular amplifier type, as seen in the case of the PMT.

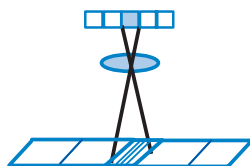


Single and Multiple Detectors

The detection principles discussed thus far have been specifically applied to single-element detectors; they are applicable to multiple element detectors as well. Array detectors may be linear or (more common in most imaging today) two-dimensional. They may be utilized with a scanner or in staring mode. A mechanical scanner provides an additional source of system noise, but the use of multiple detectors increases SNR by the square root of the number of detectors, $SNR_{new} = SNR_{old} \times N^{1/2}$. Point sources underfill the FOV of an individual detector element (**pixel**), whereas extended sources overfill it.



This **instantaneous field of view (IFOV)** is often measured in micro-radians for many of today's high-performance imagers, and it determines a system's spatial resolution. For instance, if the IFOV is 3 μ rad and the system is at 300 km altitude, the spatial resolution is 0.9 m on the ground.



Single Detector

Information gathered from one λ band or FOV at one time

Simple electronic interface

Complex scanning scheme needed due to one detector

One detector, one response

Multiple Detectors

Simultaneous measurements possible

More complex electronics due to array format

Simple scan or no scan requirement if a staring array

Magnitude of response can vary over the array due to responsivity nonuniformities between pixels

Detector Array Architectures

Further tradeoffs may be made among array technologies, including CCD, CMOS, and CID. **Charge-coupled device (CCD)** technology achieves arrays with large numbers of pixels and allows efficient charge transfer to the array output. **CMOS (complementary metal-oxide semiconductor)** structures cost less than CCDs to manufacture and exhibit high yields. **Charge-injection devices (CIDs)** employ pixels that may be addressed individually. They may be used to stare at scenes for long periods without charge spillover (“blooming”) into adjacent pixels.

	CCD	CID	CMOS
Array fill factor	100% possible	80% or better	Varies: 30%–100%
Sensitivity	Highest	High when integrating frames	Not as high as CCD
Pixel-to-pixel uniformity	High	Not as high as CCD	Can be high for on-chip processing
Blooming control	Can be a problem	Excellent	Can be improved
Fabrication	Requires specialized processing	Uses standard CMOS processing	Uses existing semiconductor fab techniques
Advantages	Well-established and characterized	Low-light level apps & excellent blooming control	Many on-chip signal processing features
Disadvantages	Blooming control	Noisy	Readouts can be noisy

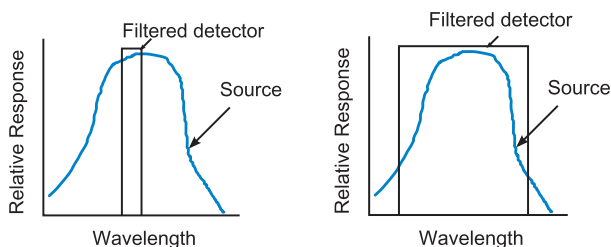
Choosing a Detector

Several practical questions arise when choosing a detector for a particular application, among them:

- Is the application imaging or non-imaging?
- What is the desired spectral resolution?
- What is the desired spatial resolution?
- What dynamic range is required?
- What is the expected temporal response of the phenomenon you wish to detect or measure?
- How do expected system size, weight, and power factor into the choice of detector?
- What is the cost of the detector (or array)?

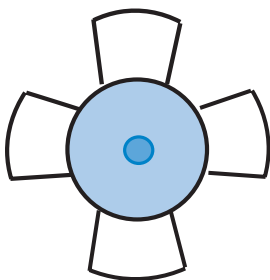
There are other questions, but these are the first that might be asked. In all cases, the first consideration should be the physical characteristics of the phenomenon under study/measurement, with practical considerations including cost constraints to follow.

Designers can err by choosing a detector that does not spectrally match the phenomenon to be measured.



In the first case, the detector's filtered response does not match the wavelength range of the source; in the second, the wavelength response is matched by the filtered detector to within a small error. However, if the goal of the project is to collect information from the source in only the small spectral region indicated in the first figure, then the first filtered detector would be a good choice.

Choppers and Radiation References

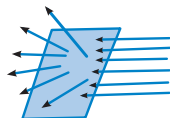


Many **choppers** are available that modulate the input signal with respect to time for detectors, including pyroelectrics. The most common are spinning blades driven by an electric motor. Choppers allow the system designer to use drift-free ac amplifiers and to avoid the $1/f$ noise region. Disad-

vantages include loss of at least 50% of the input power, the addition of noise both electronic and acoustic, and the possibility of unintended reflection from blades absent proper coating for the wavelength region in which the chopper operates.

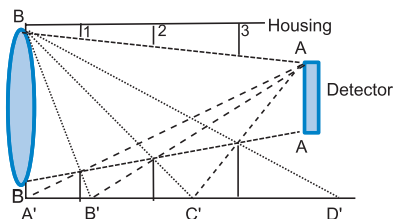
The fraction of radiant power available to the detector or system after chopping may be calculated as the **chopping factor** F_c , which is waveform dependent—for a square wave input, it is about 0.45, and for a sine wave input (most common), it is about 0.35.

Radiation reference sources may be contained within an instrument or in the instrument's environment (test setup or flight platform). They are of two kinds: (1) internal calibration sources and (2) references whose known properties allow the correct target signal to be deduced. In (2), $\text{Correction Factor} = \text{Signal}_{\text{target}} - \text{Signal}_{\text{ref}}$, where $\text{Signal}_{\text{target}}$ is the uncorrected target signal and $\text{Signal}_{\text{ref}}$ is the internal reference signal. The correction factor is then algebraically added to the target signal to produce the corrected output. Ideally, the reference signal should be from a source very similar in radiative character to the desired target. In the infrared, references include a blackbody or a blackened or reflective chopper. **Solar diffusing panels** may be used as radiation references and as on-board calibrators in the solar-reflective wavelength region (VIS–NIR particularly).



Baffles and Cosine Correctors

Baffles are mechanical structures within an instrument that reject out-of-field radiation from stray-light sources. In the best circumstances, baffles are arranged so that the detector does not “see” directly illuminated surfaces.

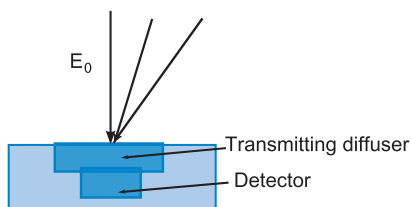


Simplified Procedure for Baffle Placement

1. Draw segments A-B (locus of aperture edges).
2. Draw A-A' (edge of detector to front corner).
3. Draw Baffle #1 (intersection of A-B and A-A').
4. Draw B-B' (edge of aperture through Baffle #1).
5. Draw A-B' (edge of detector to front aperture shadow).
6. Draw Baffle #2 (intersection of A-B and A-B').
7. Repeat.

Baffle materials should be specular, as the goal is to define exactly where the stray light is heading.

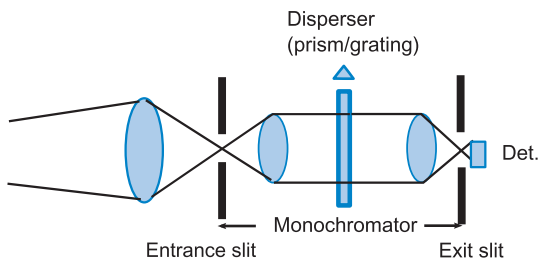
Cosine correctors accept radiation from a wide angular range, enhancing the spatial capabilities of a receiver, fiber optic probe, or detector head. The desired result for this transmitting diffuser is to approach $E = E_0 \cos \theta$ as closely as possible, where θ is the angle between the surface normal and incoming radiation, and E_0 is irradiance at normal incidence.



Spectral Separation Mechanisms

Spectral instruments employ a dispersive element to separate component wavelengths of incoming optical radiation. Two of the most common are **spectrometers** and **spectroradiometers**, the former providing a wavelength-dependent distribution of incoming signal and the latter anchoring that distribution to a specific radiometric quantity (such as irradiance).

The heart of the instrument is the **monochromator** with its dispersing element. **Prisms** and **gratings** are the most common dispersers, but others are used as well.

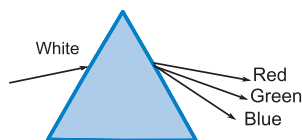


Spectroradiometers are characterized in terms of **resolving power** Q_{rp} and throughput. The resolving power relates a physical parameter of the disperser to $\lambda d\lambda$, where λ is the center wavelength of a band, and $d\lambda$ is the minimum wavelength separation for two line sources calculated according to the **Rayleigh criterion**, $1.22\lambda(f/\#)$. Expressions for throughput include the area of the entrance slit and the projected area of the disperser.

Do not overfill the spectrometer slit—there is no advantage in throughput to be gained, and the disadvantage of possible stray-light effects exists.

Spectroradiometers may employ either single detectors or arrays at the focal plane; there are advantages and disadvantages to each approach.

Prisms and Gratings

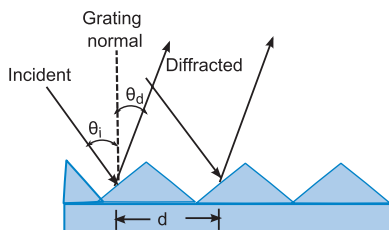


For a prism-based instrument, $Q_{rp} = \lambda/d\lambda = bdn/d\lambda$, where b is the length of the prism base and $dn/d\lambda$ is the change in the prism's refractive index as a function of wavelength. Throughput T is

$$A\Omega = (A_{slit}A_{prism} \cos \theta)/f^2$$

where the area of the slit is normal to the optical axis, the $\cos \theta$ factor accounts for the projected area of the prism, and f is the focal length of the focusing optical element.

A grating spectrometer obeys the **grating equation**, $m\lambda = d(\sin \theta_i + \sin \theta_d)$, where λ is the wavelength of optical radiation, θ_i is the angle of incidence, θ_d is the angle of diffraction, and d is the spacing between grooves. The integer m is the **order number**, which accounts for the periodicity of the diffracted waveform resulting in multiple diffraction patterns at each wavelength. Resolving power of a grating instrument is $Q_{rp} = mN$, where N is the number of grooves illuminated. The throughput expression is similar to that of a prism instrument: $T = (A_{slit}A_{grating} \cos \theta)/f^2$. In this case, θ also refers to the angle between the optical axis and grating normal.



Throughput

Efficiency

Monochromaticity

Dispersion ($d\theta_d/d\lambda$)

Bandwidth (fixed slit)

Prism

Low

~ Constant

Single λ

Nonlinear

Narrow in
blue, wide in
red

Grating

Higher

Strongly peaked

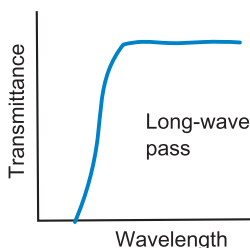
Multiple orders

Linear

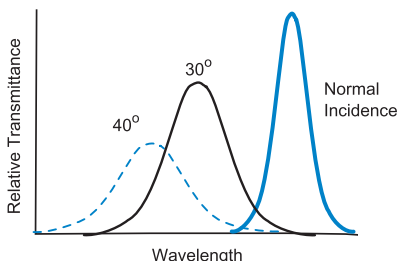
Constant

Filters

Filters may be used to provide spectral selection in a radiometric instrument. They do so by passing some wavelengths while rejecting others. **Thin film interference filters** are common for this purpose. They function as optical resonant cavities that permit only certain wavelengths to be transmitted when irradiated by a broadband source. When deployed off normal, their passband shifts and broadens, providing a reduced peak at a shorter wavelength.



Absorption filters constructed of gels or glass also provide spectral selection, although they typically have larger bandwidths than the narrowest interference filters. As the angle of incidence of incoming radiation is increased, they are not as prone as interference filters to change in the cut-on and cut-off wavelengths. Both absorption and interference filters can be used in a filter wheel to provide a (discontinuous) source spectrum, with each filtered channel providing one spectral value.



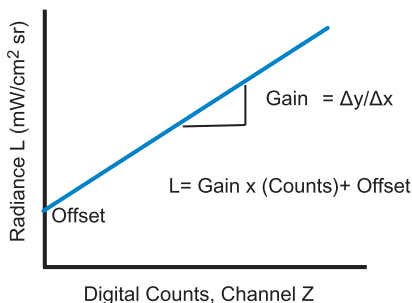
Neutral density (ND) filters attenuate an incoming signal. They find many uses in photography to reduce the illuminance of a scene and are also used in scientific applications. The relationship between filter number and attenuation is

$$n = -\log(E_{\text{filtered}}/E_{\text{incident}})$$

For example, filter ND 2 reduces signal irradiance by a factor of 100.

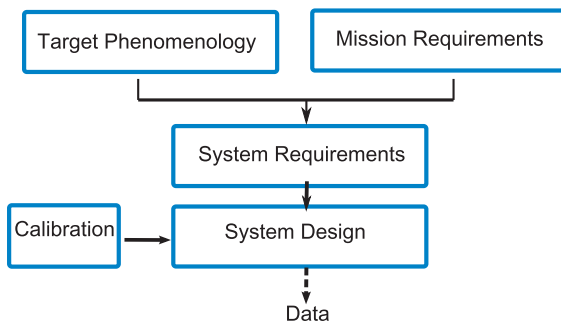
Radiometric Calibration Basics

Radiometric systems are calibrated to tie the system's output signal (a digital count value, voltage, or current) to an input quantity such as radiance, irradiance or (less often) optical power. Calibrations may be **absolute**—



example—or **relative**, relying on correlation between detector responses in an array, dataset characteristics, features in a scene, or other parameters.

In the absolute case, the calibration curve associates sensor output with a specific radiometric input.



It is always desirable to make the calibration equation as simple as possible—a wide, linear range of response is preferred.

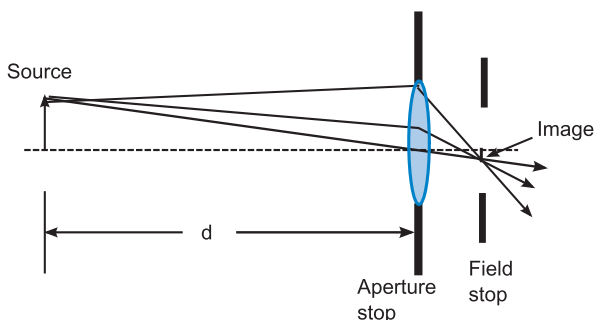
It is good engineering practice to develop the calibration scheme at the beginning of the design process; too often, it is considered only after the system design is finalized.

Radiometric Calibration Philosophy

The most general principle is to calibrate a system in the manner it will be used. For example, if a distant point source is to be measured, a point-source irradiance calibration is the most desirable. However, depending on instrument conditions and test equipment available, a good result might also be obtained by a radiance calibration corrected for the instrument's solid angle. The following list describes some basic principles:

- Calibration requirements are driven by science and engineering goals.
- Make the calibration as independent of the specific instrument as possible.
- Account for every factor influencing the calibration.
- Select appropriate calibration standards.
- Conduct an error assessment during the planning phase to allow accurate estimation of data uncertainties.
- End-to-end calibration is preferred to summation of individual, component-level calibrations.
- Vary relevant external parameters (temperature, pressure, humidity, etc.) to determine their influence on the calibration transfer function.
- Determine the calibration transfer function over the entire dynamic range of the instrument.
- Use more than one calibration configuration, if possible, and compare results for consistency.
- Prior to the calibration of a flight instrument, conduct the entire procedure on a test dummy, prototype, or engineering model to uncover and fix any problems with equipment or procedures.
- Inspect and interpret results early, while the instrument is still in the test position; this allows for immediate correction to equipment and procedures.
- Because calibration is often the last step on a GANTT chart prior to instrument delivery, it is most susceptible to the “squeeze play.” Plan ahead!
- Adhere to the KISS (Keep It Simple, Smarty!) principle as much as possible.

Distant Small Source Calibration



In a **distant small source calibration**, the inverse square law applies. This is an irradiance calibration in which the relationship between output and input signals is expressed as

$$\mathfrak{R}_E = \text{Signal} \times (d^2/I)$$

where

\mathfrak{R}_E = **irradiance responsivity** [Signal/(W/m²)]

d = source–system distance (m)

I = source intensity (W/sr)

The primary advantage of this calibration method is that almost any source can be used, provided it is both “small” and “distant” enough to meet the inverse square law test.

There are several disadvantages, however:

- Signals are typically small.
- There may be an intervening atmosphere.
- Distance d must be known well (the error in \mathfrak{R}_E is twice the error in d due to the square term).
- A background is present due to the fact that the source image often does not fill the instrument’s field stop.

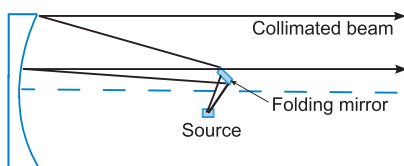
Examples of sources used in this method include black-body radiation simulators, small tungsten lamps used at suitable distances, and the sun and stars.

Collimators and the Distant Small Source

Collimators—reflective and refractive—can improve the distant small source calibration when a laboratory source is placed at the collimator focal point. The source image must, as above, be contained within the instrument's field stop. An off-axis parabola is often used for this purpose. In this case, the irradiance responsivity is

$$\mathcal{R}_E = \text{Signal} \times (f^2/I)$$

where f is the collimator focal length.



Advantages:

- A controllable atmosphere (laboratory)
- Controllable background
- Possible use of nearly any small source
- Larger signals than astronomical sources provide

Disadvantages:

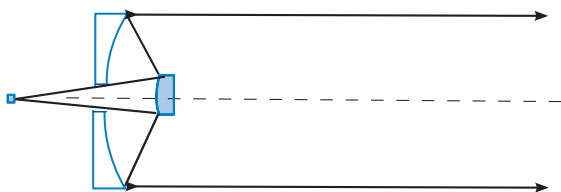
- Must know the focal length f (typically a one-time measurement)
- Hardware can be expensive, both for collimator optics and any chamber hardware (vacuum, for cooled, low-background infrared targets) in which they might be encased

A reflective on-axis collimator (centrally obscured system such as a Cassegrain) may also be used. The responsivity equation is the same as above, as are the advantages.

Disadvantages:

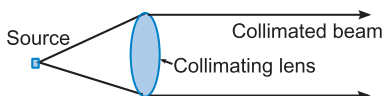
- Presence of central obscuration
- Diffraction possible from secondary mirror mount
- A direct path into the collimator for source stray light
- Difficulties in baffling

More on Collimators



The on-axis reflective system provides the advantage of accommodating instruments with wide fields of view. As with the off-axis parabola, advantages and disadvantages will vary with instrument and application.

The **refractive collimator** provides an alternative to a mirror-based system.



Advantages:

- Relatively simple alignment (in the visible region) due to an unfolded path
- Simple to set up, particularly if off-the-shelf components are used

Disadvantages:

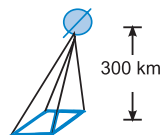
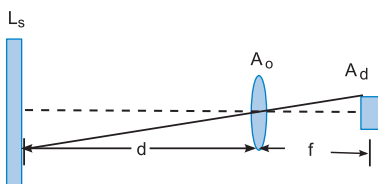
- Wavelength range limited by $\tau(\lambda)$ of the material
- Reflection losses due to refractive index
- Ghost images due to reflections from optical elements
- Wavelength dependence of anti-reflection coatings
- Chromatic aberration from refractive optical elements
- Possible difficulties in alignment if the lens is transmissive

The good news: many of these difficulties can be dismissed or minimized if the collimator is used in the wavelength region for which it was optimized.

Extended Source Calibrations

For calibration purposes, **extended sources** are of two types, **near** and **distant**. Radiance from the near extended source must fill the instrument's aperture stop in addition

to its field stop. In the distant extended source case, which is often used by satellite or airborne instrumentation with respect to a large, uniform ground target, atmospheric correction is required. The **radiance responsivity** for both cases is $\mathfrak{R}_L = \text{Signal}/L$, where \mathfrak{R}_L is in $\text{Signal}/(\text{W}/\text{m}^2\text{sr})$.



Advantages:

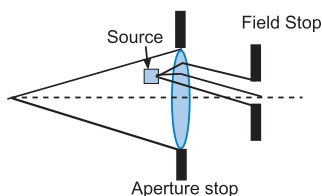
- Distance d between source and radiometer is not important.
- There is no background (assuming proper test setup).
- If the instrument is not precisely aligned (detector not exactly at distance f from aperture), it doesn't matter.
- There is minimal intervening atmosphere (in the near extended source case).

The presence of an intervening atmosphere is a disadvantage in the distant extended-source case; and in both cases, a large uniform source is required. Laboratory sources may include a blackbody radiation simulator, an integrating sphere, or a transmissive or reflective diffuser with a standard lamp. Uniform natural sources, such as large-area sites at White Sands, New Mexico, are among the distant extended sources used.

Radiative transfer programs used for atmospheric correction include MODTRAN (son of LOWTRAN), FASCODE, and SMARTS in the US, and 5S and 6S in France.

Other Calibration Methods

The **near small source (Jones source)** calibration method provides radiance responsivity and includes the ratio of instrument aperture and source areas, $\mathfrak{R}_L = \text{Signal}/L_s \times (A_o/A_s)$ with units in $\text{Signal}/(\text{W}/\text{m}^2 \text{ sr})$. The instrument is focused at infinity. Radiation from the small source placed within the cone will fill the instrument's field stop, but not its aperture, hence the need for the ratio.



Advantages:

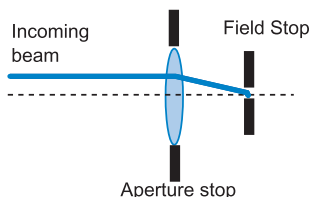
- Minimal atmosphere
- Calibration source can be small

Disadvantage:

- Need to account for background radiation

This is a good method to use for some ground-based astronomical telescopes, as the small source can be mounted to the side of the telescope and positioned in front of the aperture in calibration mode.

In the **direct method**, a power responsivity \mathfrak{R}_Φ in Signal/W is obtained by pointing a small, narrow beam of known flux at a radiometer whose aperture and field stops will be underfilled. A laser beam is often used in this method.



Advantage:

- Simple setup

Disadvantages:

- Presence of background radiation
- No accounting for aperture or field stop nonuniformities

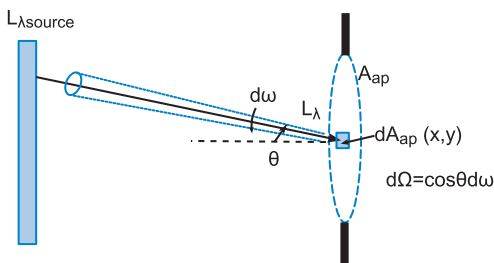
The Measurement Equation

The **measurement equation** relates an instrument's output signal to input radiometric quantity (radiance, irradiance, flux) as a function of instrument responsivity. One version, in differential form, is

$$d\text{Signal} = \mathfrak{R}(\lambda)_{\text{world}} L_{\lambda \text{ world}} dA d\Omega d\lambda$$

where the usual suspects of spectral radiance, element of area, and element of projected solid angle have been discussed at length; $\mathfrak{R}(\lambda)$ is the instrument's spectral responsivity at a particular wavelength; and "world" refers to the environment surrounding the measurement, which includes:

θ, ϕ (angular dependence); x, y (position dependence); t, ν (time, frequency); s, p (polarization components); along with diffraction, instrument and test setup nonlinearities, and "phase of the moon."



In terms of an integral, the above equation looks like

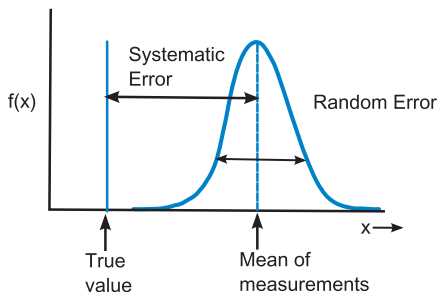
$$\text{Signal} = \iiint \mathfrak{R}(\lambda) L_{\lambda} dA_{\text{ap}} d\Omega d\lambda$$

where L_{λ} is input spectral radiance, related to source spectral radiance by the transmission of the intervening medium. Other forms of the measurement equation exist and may be formulated with respect to measurement configuration. For a point source, where I_{λ} is the point source's spectral intensity and d is the source–aperture distance,

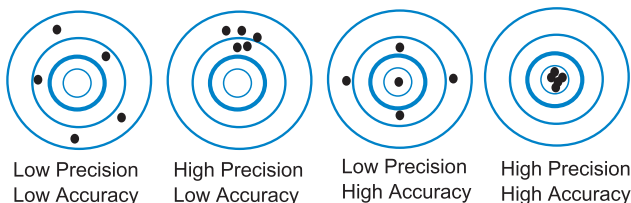
$$\text{Signal} = 1/d^2 \iint \mathfrak{R}(\lambda) I_{\lambda} dA_{\text{ap}} d\lambda$$

Errors in Measurements

Measurement errors are of two types: random and systematic. **Random errors** are those that vary in an unpredictable manner when the same quantity is measured repeatedly under identical conditions. **Precision** is a term associated with random error; a measurement is considered precise if it is repeatable. A normal, Gaussian distribution of random error is typically assumed. To reduce the value of random error, increase the number of measurements and apply statistical analysis to the result.



Systematic errors constitute a displacement between a quantity's measured value and its true value. **Accuracy** is often used in discussion of systematic errors, many of which arise from improper calibration and/or test setup. Unlike random errors, systematic errors are not revealed by repeated measurement.



In the third case above, the x - y average of the pattern lies very close to the target center. Systematic and random errors must be considered together in evaluating a measurement's total uncertainty. Errors can be specified as absolute, with the magnitude in appropriate engineering units, or fractionally, usually in percent.

Signal-to-Noise Ratio and Measurement Error

The fundamental limit to a measurement error is random noise. If all other error sources are reduced to zero, the remaining noise is most likely to be Gaussian, usually shot noise or Johnson noise associated with the detector. In such a system, the measurement uncertainty is inversely related to SNR: *Measurement uncertainty* = $(1/\text{SNR})$.

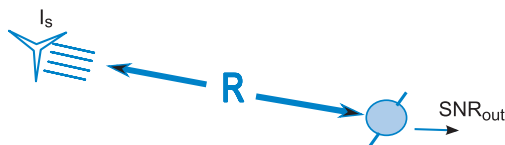
SNR (single measurement)	Uncertainty
1	1 (100%)
10	0.1 (10%)
100	0.01 (1%)
1000	0.001 (0.1%)

Taking repeated measurements improves SNR. The resultant SNR is proportional to the square root of the number of independent measurements, $\text{SNR} \propto \sqrt{N}$. Further analytical tools help with the dataset analysis.

Tool	Formula
Mean	$\bar{x} = \frac{\sum_i x_i}{N}$, N = number of measurements
Variance	$\sigma^2 = \frac{\sum_i (x_i - \bar{x})^2}{N - 1}$
Standard deviation	$\sigma = \sqrt{\sigma^2}$
Standard deviation of mean	$\sigma_{\bar{x}} = \frac{\sigma}{\sqrt{N}}$

An important contribution to random error (precision) is the granularity of the measurement instrument. Most electrical readings are now taken with digital instrumentation. In this case, quantization noise may be calculated as $LSB = (\text{Signal}_{max})/2^n$, where Signal_{max} is the full-scale signal, LSB is the magnitude of the least significant bit, and n is the number of bits.

The Range Equation



The **range equation** provides the distance at which a specified target will generate a particular SNR ratio from a passive electro-optical system whose parameters are specified. Its components can be separated into four categories:

$$R = \underbrace{(I_s \tau_a)}_1 \times \underbrace{\left[\frac{\pi}{4} \frac{D_o \tau_o}{(f/\#) \sqrt{\Omega}} \right]}_2^{1/2} \times \underbrace{(D^*)}_3^{1/2} \times \underbrace{\left(\frac{1}{SNR \sqrt{B}} \right)}_4^{1/2}$$

Category

1: Target

2: Optical system

3: Detector

4: Signal processing

Includes

Source intensity, intervening atmosphere transmission

Receiver diameter D_o , $f/\#$, solid angle FOV, optics transmission

D^*

Required SNR and noise bandwidth

The range equation can be permuted to calculate the expected SNR for a specified target range.

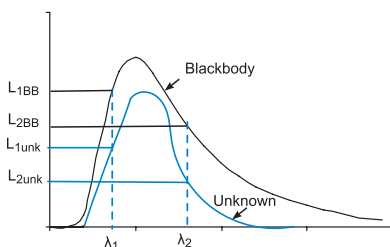
Several other equations exist for assessing the performance of imaging and non-imaging systems as a function of several parameters. For example, the **noise equivalent irradiance (NEI)** for a target that underfills an instrument's FOV is

$$NEI = \frac{4(f/\#)\Omega^{1/2}B^{1/2}}{\pi D_o D^* \tau_o}$$

Radiometric Temperatures

A number of temperature terms are used in radiometry and photometry; the definitions below refer to an object whose temperature is unknown. The object's **radiation temperature** is the temperature of a blackbody having the same total radiance as the unknown. Its **radiance temperature (brightness temperature)** is the temperature of a blackbody that has the same radiance in a narrow spectral band as the unknown.

The object's **ratio temperature** is the temperature of a blackbody with the same ratio of radiances at two wavelengths as the unknown:



$$\frac{L_{\lambda 1BB}}{L_{\lambda 2BB}} = \frac{L_{\lambda 1unknown}}{L_{\lambda 2unknown}}$$

The **distribution temperature** is the temperature of a blackbody whose radiance values, over a significant portion of the spectrum, are most nearly proportional to those of the unknown. Mathematically, it is the temperature of the blackbody for which the following integral is minimized by successive selections of the constant a and temperature T (M'_{λ} is the measured test source exitance):

$$\int_{\lambda_1}^{\lambda_2} [1 - (M'_{\lambda}/aM_{\lambda}(T))]^2 d\lambda$$

An object's **color temperature** is the temperature of a blackbody having the same chromaticity (color) as the unknown. In many applications, **correlated color temperature (CCT)**, the temperature of a blackbody having the most similar chromaticity, is used instead.

Sun	5750 K	$\lambda_{peak} = 0.5 \mu\text{m}$
Tungsten lamp	3000 K	$\lambda_p = 1 \mu\text{m}$
Earth	300 K	$\lambda_p = 10 \mu\text{m}$

Photometric Quantities

Photometry is a subset of radiometry in which the input optical stimulus is modified by the response of the human eye. Its basic quantities are defined similarly to radiometric quantities, with subscript v (for visual) added.

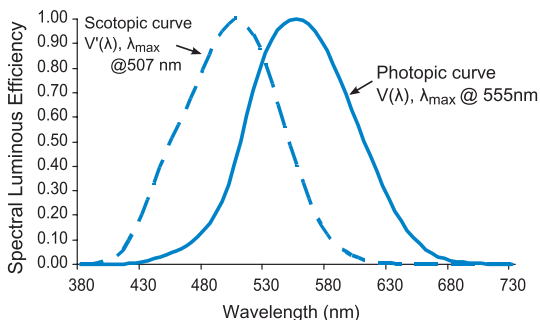
Quantity	Symbol	Definition	Units
Luminous energy	Q_v	—	$\text{lm} \cdot \text{s}$
Luminous power	Φ_v	$\frac{dQ_v}{dt}$	lm
Luminous intensity	I_v	$\frac{d\Phi_v}{d\omega}$	lm/sr (cd)
Luminous exitance	M_v	$\frac{d\Phi_v}{dA}$	lm/m^2
Illuminance	E_v	$\frac{d\Phi_v}{dA}$	lm/m^2
Luminance	L_v	$\frac{d^2\Phi_v}{dAd\omega\cos\theta}$	$\text{lm/m}^2\text{sr (cd/m}^2\text{)}$

Lumens/m² (lm/m²) are also called *lux* (lx); lm · s (a unit of energy) is also called *talbot*.

The *candela* (cd) is one of seven SI base quantities from which other quantities are derived: “The candela is the luminous intensity, in a given direction, of a source that emits monochromatic radiation of frequency 540×10^{12} Hz and that has a radiant intensity in that direction of $1/638 \text{ W sr}^{-1}$ ” [see Ref. 3]. Note that the wavelength corresponding to the given frequency is 555 nm.

Human Visual Response

The dynamic range of human vision is about 11 orders of magnitude, but the eye's spectral response is confined to a narrow region of the electromagnetic spectrum. Two important curves ("efficiency functions") defined by the CIE represent the "light-" and "dark-adapted" eye functions—the **photopic** and **scotopic curves**, respectively.



Each curve features a response by one of the two types of visual photoreceptors, **rods** and **cones**—the cones responding to photopic conditions and the rods to scotopic. The “in-between” state of illumination, where both rods and cones respond, is called **mesopic**.

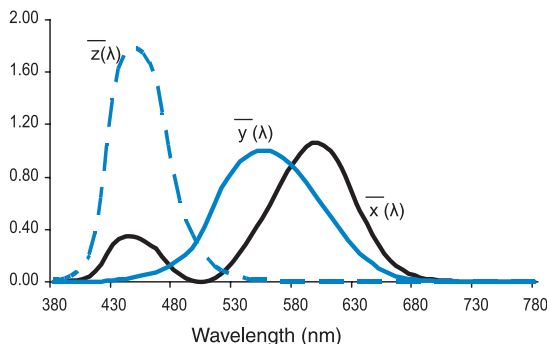
In order to solve problems in photometry with data acquired from radiometric instruments, the radiometric distribution, for example, power, must be folded into an integral with the $V(\lambda)$ function over the photopic limits (for light adaptation):

$$\Phi_v = K_m \int_{380}^{760} V(\lambda) \Phi_\lambda d\lambda$$

Similar formulations apply for M_v , I_v , etc. The constant K_m is called the **luminous efficacy**; its value is 683 lm/W at 555 nm. For the scotopic curve, the formulation is similar with Φ'_v replacing Φ_v , and $V'(\lambda)$ replacing $V(\lambda)$. The constant is K'_m , whose value is 1700 lm/W at 507 nm. The units of both Φ_v and Φ'_v are lumens.

Color

The eye's cones provide the capability for color vision, with three curves called **color matching functions** that describe the response of the **CIE Standard Observer**. The 1931 CIE Standard Observer employs a 2-deg FOV, with $\bar{y}(\lambda) = V(\lambda)$.



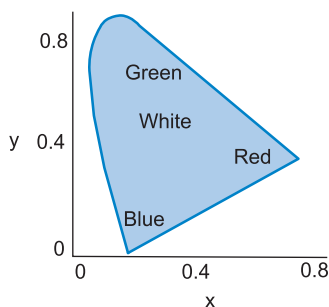
The three curves allow calculation of the **tristimulus values** X , Y , and Z that completely describe a test color in terms of the three primaries—red, green, and blue:

$$X = K_m \int_{380}^{760} \Phi_{\lambda} \rho(\lambda) \bar{x}(\lambda) d\lambda \quad Y = K_m \int_{380}^{760} \Phi_{\lambda} \rho(\lambda) \bar{y}(\lambda) d\lambda$$

$$Z = K_m \int_{380}^{760} \Phi_{\lambda} \rho(\lambda) \bar{z}(\lambda) d\lambda$$

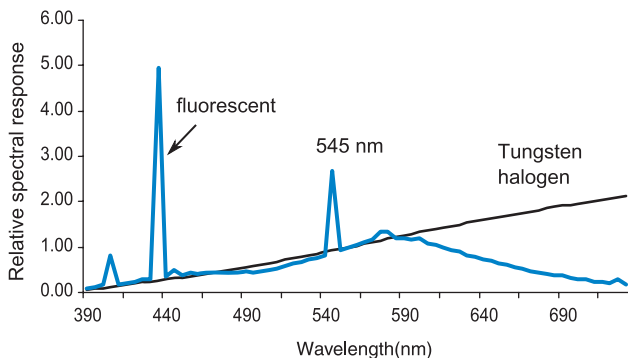
Φ_{λ} is incident radiant power, $\rho(\lambda)$ is spectral reflectance, and $K_m = 683 \text{ lm/W}$.

Normalizing these values by $(X + Y + Z)$ gives the **chromaticity coordinates** x , y , and z ($z = 1 - x - y$), which specify any color in 2D space via the 1931 CIE chromaticity diagram, whose general shape is indicated here.

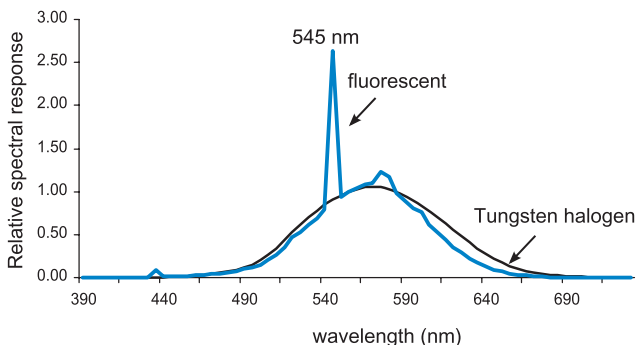


Sources and the Eye's Response

It is instructive to consider the spectral distribution from the product of a source function and the eye's response to light. Data taken with a USB spectrometer and plotted at 5-nm increments, with response normalized to 1 at 555 nm, show the peaks from a typical fluorescent office light or compact fluorescent light (CFL) bulb against the smooth function of a laboratory tungsten-halogen incandescent source.



When the photopic curve is applied to the data, the peak at 545 nm stands out as the most prominent fluorescent feature, the larger peak at 435 nm having been minimized by the eye's response. Before choosing a source, be sure to understand its response on the chosen detector.



SI Base Quantities, Prefixes, and Uncertainty Reporting

SI Base Quantities

Quantity	Name	Symbol
length	meter	m
mass	kilogram	kg
time	second	s
electric current	ampere	A
thermodynamic temperature	kelvin	K
amount of substance	mole	mol
luminous intensity	candela	cd

SI Prefixes

Factor	Prefix	Symbol	Factor	Prefix	Symbol
10^{18}	exa	E	10^{-1}	deci	d
10^{15}	peta	P	10^{-2}	centi	c
10^{12}	tera	T	10^{-3}	milli	m
10^9	giga	G	10^{-6}	micro	μ
10^6	mega	M	10^{-9}	nano	n
10^3	kilo	k	10^{-12}	pico	p
10^2	hecto	h	10^{-15}	femto	f
10^1	deka	da	10^{-18}	atto	a

Concise Notation and Uncertainty Reporting

The **absolute uncertainty** of a measurement is its estimated standard deviation σ , such that, for an approximately Gaussian distribution of error, 68% of the measured value falls within the limits of the value $\pm 1\sigma$. For example, the absolute uncertainty in the value of c_2 , 0.014387752 m K, is 0.000000025 m K; the expression becomes $1.4387752 \times 10^{-2} \pm 0.000000025$ m K. The constant and its standard deviation may also be expressed in **concise notation** as $1.4387752(25) \times 10^{-2}$ m K, where the (25) refers to the corresponding last digits of the constant.

A **relative uncertainty** may be expressed. This is the absolute uncertainty divided by the value of the constant. In the case of c_2 , it is 1.7×10^{-6} . The entire expression is then $c_2 = 1.4387752(25) \times 10^{-2}$ m K (1.7×10^{-6}).

Physical Constants: 2010 CODATA Recommended Values

Quantity	Symbol	Value	Units	Relative uncertainty
Speed of light (vacuum)	c, c_0	299,792,458	m/s	exact
Magnetic constant	μ_0	$4\pi \times 10^{-7}$	N/A ²	exact
Electric constant ($1/\mu_0 c^2$)	ϵ_0	$8.854187... \times 10^{-12}$	F/m	exact
Planck constant	h	$6.62606957 (29) \times 10^{-34}$	J s	4.4×10^{-8}
Electronic charge	q, e	$1.602176565 (35) \times 10^{-19}$	C	2.2×10^{-8}
Boltzmann constant	k	$1.3806488 (13) \times 10^{-23}$	J/K	9.1×10^{-7}
Boltzmann constant	k	$8.6173324 (78) \times 10^{-5}$	eV/K	9.1×10^{-7}
Stefan–Boltzmann constant	σ	$5.670373 (21) \times 10^{-8}$	W/(m ² K ⁴)	3.6×10^{-6}
First radiation constant ($2\pi\hbar c^2$)	c_1	$3.74177153 (17) \times 10^{-16}$	W m ²	4.4×10^{-8}
First radiation constant for L_λ	c_{1L}	$1.191042869 (53) \times 10^{-16}$	Wm ² /sr	4.4×10^{-8}
Second radiation constant ($\hbar c/k$)	c_2	$1.4387770 (13) \times 10^{-2}$	m K	9.1×10^{-7}
Wien displacement law constant	b	$2.8977721 (26) \times 10^{-3}$	m K	9.1×10^{-7}

Source Luminance Values

Astronomical Sources

Source	Luminance (cd/m²)
Night sky, cloudy, no moon	10^{-4}
Darkest sky	4×10^{-4}
Night sky, clear, no moon	10^{-3}
Night sky, full moon	10^{-2}
Clear sky 0.5 h after sunset	0.1
Clear sky 0.25 h after sunset	1
Cloudy sky at sunset	10
Gray sky at noon	10^2
Cloudy sky at noon	10^3
Moon	2.5×10^3
Average clear sky	8×10^3
Clear sky at noon	10^4
Solar disc	1.6×10^9
Lightning	8×10^{10}

Practical Sources

Source	Luminance (cd/m²)
Minimum of human vision	3×10^{-6}
Scotopic vision valid	<0.003
Photopic vision valid	>3
Green electroluminescent	25
T8 cool white fluorescent	10^4
Acetylene burner	10^5
60 W inside frosted lamp	1.2×10^5
Candle	6×10^5
Sodium vapor lamp	7×10^5
High-pressure Hg vapor lamp	1.5×10^6
Tungsten lamp filament	8×10^6
Plain carbon arc crater	1.6×10^8
Cored carbon arc crater	10^9
Atomic fusion bomb	10^{12}

More Source Values

Illuminance of Various Sources

Source	Illuminance ($\text{lm/m}^2 = \text{lux}$)
Absolute minimum for visual magnitude, $M_v = 8$	1.6×10^{-9}
Typical minimum, $M_v = 6$	10^{-8}
0-magnitude star outside the atmosphere	2.54×10^{-6}
Venus	1.3×10^{-4}
Full moonlight	1
Street lighting (typical)	10
Recommended reading	10^2
Workplace lighting	10^2 – 10^3
Lighting for surgery	10^4

Luminous Intensity Values

Source	Luminous intensity (cd)
Bicycle headlamp without reflector, any direction	2.5
Bicycle headlamp with reflector, center of beam	250
Incandescent reflector lamp, PAR38E Spot, 120 W, center of beam	10^4
Lighthouse, center of beam	2×10^6

Astronomical Conversion Factors

1 Jansky (Jy)	$10^{-26} \text{ W/m}^2 \text{ Hz}$ (spectral irradiance)
1 $\text{W/cm}^2 \cdot \mu\text{m}$	$3 \times 10^{16}/\lambda^2 \text{ Jy}$
1 Rayleigh	$10^6 \text{ photons/cm}^2 \text{ s}$
1 S_{10} (number of 10^{th} magnitude stars per square degree)	$1.23 \times 10^{-12} \text{ W/cm}^2 \text{ sr } \mu\text{m at}$ $0.55 \mu\text{m}$
1 S_{10}	$1.899 \times 10^6 \text{ photons/s cm}^2 \text{ sr } \mu\text{m}$ $\text{at } 0.55 \mu\text{m}$

Solid Angle Relationships

$\Theta_{1/2}$ (deg)	$\Theta_{1/2}$ (rad)	ω (sr)	Ω (sr)	ω/Ω	$f/\#$
0.573	.0100	.00031	.00031	1.000	50.00
1.000	.0175	.00096	.00096	1.000	28.65
1.146	.0200	.00126	.00126	1.000	25.00
1.719	.0300	.00283	.00283	1.000	16.67
2.000	.0349	.00383	.00383	1.000	14.33
2.292	.0400	.00503	.00502	1.000	12.50
2.865	.0500	.00785	.00785	1.001	10.00
3.000	.0524	.00861	.00861	1.001	9.554
4.000	.0698	.0153	.0153	1.001	7.168
5.000	.0873	.0239	.0239	1.002	5.737
5.730	.1000	.0314	.0313	1.003	5.008
10.00	.1745	.0955	.0947	1.008	2.880
11.46	.2000	.1252	.1240	1.010	2.517
15.00	.2618	.2141	.2104	1.017	1.932
17.19	.3000	.2806	.2744	1.023	1.692
20.00	.3491	.3789	.3675	1.031	1.462
22.92	.4000	.4960	.4764	1.041	1.284
25.00	.4363	.5887	.5611	1.049	1.183
28.65	.5000	.7692	.7221	1.065	1.043
30.00	.5236	.8418	.7854	1.072	1.000
34.38	.6000	1.097	1.002	1.096	0.886
40.11	.7000	1.478	1.304	1.133	0.776
45.00	.7854	1.840	1.571	1.172	0.707
45.84	.8000	1.906	1.617	1.179	0.697
51.57	.9000	2.377	1.928	1.233	0.638
57.30	1.000	2.888	2.224	1.298	0.594
60.00	1.047	3.142	2.356	1.333	0.577
71.63	1.250	4.269	2.830	1.521	0.527
85.95	1.500	5.839	3.126	1.868	0.501
90.00	1.571	6.283	3.142	2.000	0.500

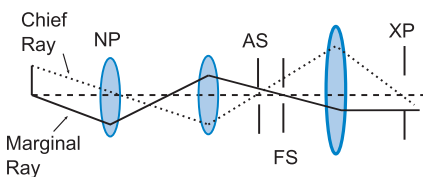
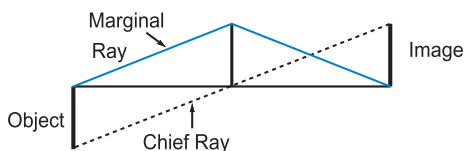
(Adapted from Ref. 4)

The percentage error using ω rather than Ω is less than 5% when $\Theta_{1/2}$ is 25 deg; less than 2% when $\Theta_{1/2}$ is 16 deg; and less than 1% when $\Theta_{1/2}$ is 10 deg.

Rays, Stops, and Pupils

The **chief ray** in an optical system originates at the edge of the object, passes through the center of the **entrance pupil (NP)**,

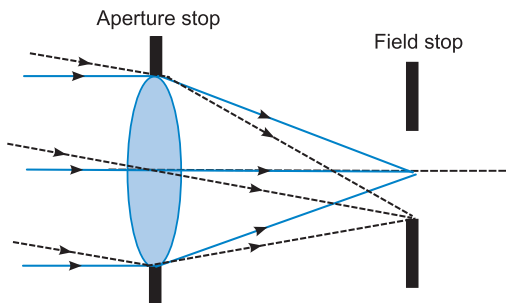
the center of the **aperture stop (AS)**, the edge of the **field stop (FS)**, and the center of the **exit pupil (XP)**. The chief ray defines image height and transverse (lateral) magnification. There may be several intermediate pupil planes in a complex optical system.



The **marginal (rim) ray** originates at the intersection of the object and optical axis. It passes through the edge of the entrance pupil, touches the edge (rim) of the aperture stop, and proceeds through the center of the field stop to the edge of the exit pupil. The marginal ray defines the system's longitudinal magnification and location of the image.

The entrance pupil is the image of the aperture stop in object space (as seen from the object), while the exit pupil is the image of the aperture stop in image space (as seen from the image).

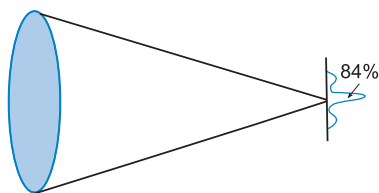
The entrance pupil is the image of the aperture stop in object space (as seen from the object), while the exit pupil is the image of the aperture stop in image space (as seen from the image).



Diffraction

In imaging applications, a point source such as a star does not image exactly to a point but creates a “blur” on the instrument focal plane. The blur arises due to the non-ideal nature of optical instrument characteristics, which result in rays being **diffracted** (bent). The effect is most pronounced for small, widely spaced apertures and longer wavelengths; hence, it can challenge designers of IR spectrometers, for example. Diffraction is less severe for shorter wavelengths and large, closely spaced apertures.

An optical system free (at least in theory) of optical aberrations is said to exhibit **diffraction-limited** performance, where the spreading of the image on the focal plane is due to diffraction effects alone.

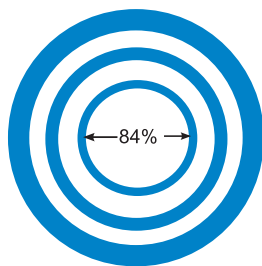


The diffraction pattern on the focal plane takes the form of the **Airy disk** which, as imaged for a circular aperture, appears as a series of

concentric rings, with 84% of the energy in the image contained in the central circle. The radius of the circle is calculated as $1.22 \lambda (f/\#)$, with $f/\#$ defined previously, and λ the wavelength of incoming optical radiation (or central wavelength of the incoming beam; the narrower, the more accurate).

Two “adjacent” objects are considered resolved, according to the **Rayleigh criterion**, when the diffraction pattern peak of object #1 falls on the first minimum (first dark ring) of object #2.

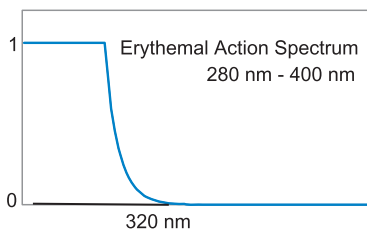
Diffraction is typically studied in depth as part of **physical optics**.



Action Spectra and Optical Radiation Regions

An **action spectrum** is a biological spectral response to an input optical stimulus. For example, action spectra describe the blue light hazard between about 400–550 nm encountered by welders, and the erythral action (skin reddening) response to UV radiation from the sun and tanning lamps.

Mathematically, the action spectrum is handled as an instrument responsivity, placed in an integral along with the input source function and integrated over the common spectral band. Depending on the phenomenon measured, multiplicative constants may also be applied to the result.



UV Band Designations—Three Separate Authorities (all wavelengths in nm)

Band	CIE	NOAA	ANSI
UVC	100–280	100–280	200–280
UVB	280–315	280–320	280–315
UVA	315–400	320–400	315–400

The UVA region is further subdivided into UVA1 and UVA2 due to differing responses to optical radiation, with UVA2 comprising 315(320) nm to 340 nm, and UVA1 extending from 340 nm to 400 nm. The erythral action spectrum is most pronounced in the UVB region. “Facultative pigmentation,” i.e., tanning, is the result of optical radiation in the UVA1.

Phototherapy in the UVA1 region of the spectrum is currently used in treatments for lupus and many skin diseases.

Equation Summary

Optical terms and basic equations

$$n = c/v \quad \lambda_0 = n\lambda$$

Snell's law:

$$n_1 \sin \theta_1 = n_2 \sin \theta_2$$

Numerical aperture:

$$NA = n \sin \Theta_{1/2}$$

$f/\#$ for object at infinity:

$$f/\# = \frac{f}{D}$$

$f/\#$ (preferred definition):

$$f/\# = \frac{1}{2 \sin \Theta_{1/2}}$$

Working $f/\#$:

$$f/\#' = (f/\#) [1 + (m/m_p)]$$

Projected area, solid angle, projected solid angle

Projected area:

$$A_p = \int_A \cos \theta dA$$

Solid angle:

$$\omega = \int_{\phi} \int_{\theta} \sin \theta d\theta d\phi$$

Solid angle of a right circular cone:

$$\omega = 2\pi(1 - \cos \Theta_{1/2})$$

Projected solid angle of a right circular cone:

$$\Omega = \pi \sin^2 \Theta_{1/2} = \frac{\pi}{4(f/\#)^2}$$

Equation Summary

Radiometric terminology and propagation laws

Radiant power:

$$\Phi = \frac{dQ}{dt}$$

Radiant intensity:

$$I = \frac{d\Phi}{d\omega}$$

Radiant exitance:

$$M = \frac{d\Phi}{dA}$$

Irradiance:

$$E = \frac{d\Phi}{dA}$$

Radiance:

$$L = \frac{d^2\Phi}{dAd\omega \cos\theta}$$

Photon flux at wavelength λ_0 :

$$\Phi_q = \Phi \frac{\lambda_0}{hc}$$

Relationship between intensity, radiance and projected area:

$$I = LA_p$$

Lambert's law:

$$I = I_0 \cos\theta$$

Lambertian approximation:

$$L(\theta, \phi) = \text{Constant}$$

Equation Summary

Lambertian surface relationships:

$$M = \pi L \quad L = \frac{E \rho}{\pi}$$

Inverse square law of irradiance:

$$E = \frac{I \cos \theta}{d^2}$$

Cosine³ law of irradiance:

$$E = \frac{I \cos^3 \theta}{d^2}$$

Cosine⁴ law of irradiance:

$$E = \frac{L A_s \cos^4 \theta}{d^2}$$

Throughput:

$$T = A \Omega$$

Basic throughput:

$$n^2 T = n^2 A \Omega$$

Equation of radiative transfer, differential form:

$$d^2 \Phi_{1 \rightarrow 2} = \frac{L(\theta, \phi) dA_1 \cos \theta_1 dA_2 \cos \theta_2}{d^2}$$

Equation of radiative transfer, integral form:

$$\Phi_{1 \rightarrow 2} = \int_{A_2} \int_{A_1} \frac{L(\theta, \phi) \cos \theta_1 \cos \theta_2 dA_1 dA_2}{d^2}$$

Configuration factor:

$$F = \frac{\Phi_{1 \rightarrow 2}}{\Phi_1}$$

Equation Summary

Radiant power gain when A_{lens} is the first surface in a system, and A_{det} is the second surface:

$$G = \frac{\tau_{lens} A_{lens}}{A_{det}}$$

Camera equation:

$$E_t = \frac{\pi L_s}{4(f/\#)^2(1+m)^2}$$

Extended source irradiance at focal plane:

$$E_t = \frac{\tau_o \tau_{atm} \pi f_v (1 - A^2) L_s(\theta, \phi) \cos^n \theta}{4(f/\#)^2(1+m)^2}$$

Point source irradiance at focal plane:

$$E_t = \frac{\tau_o \tau_{atm} f_v (1 - A^2) I_s \cos^n \theta}{d^2}$$

Simplification of the equation of radiative transfer:

$$\Phi = LA\Omega$$

Resulting irradiance on area A:

$$E = \Phi/A$$

Material properties

Total transmittance:

$$\tau = \frac{\Phi_t}{\Phi_i} = \frac{\int_0^\infty \tau(\lambda) \Phi_{\lambda i} d\lambda}{\int_0^\infty \Phi_{\lambda i} d\lambda}$$

Total reflectance:

$$\rho = \frac{\Phi_r}{\Phi_i} = \frac{\int_0^\infty \rho(\lambda) \Phi_{\lambda i} d\lambda}{\int_0^\infty \Phi_{\lambda i} d\lambda}$$

Equation Summary

Total absorptance:

$$\alpha = \frac{\Phi_a}{\Phi_i} = \frac{\int_0^\infty \alpha(\lambda) \Phi_{\lambda i} d\lambda}{\int_0^\infty \Phi_{\lambda i} d\lambda}$$

Total emittance:

$$\varepsilon = \frac{\iiint \varepsilon(\theta, \phi; \lambda) L_{\lambda BB} \sin \theta \cos \theta d\theta d\phi d\lambda}{(\sigma/\pi) T^4}$$

Spectral emittance:

$$\varepsilon(\lambda) = L_{\lambda(\text{source})} / L_{\lambda BB}$$

BRDF:

$$f_r(\theta_i, \phi_i; \theta_r, \phi_r) = \frac{dL_r(\theta_r, \phi_r)}{dE_i(\theta_i, \phi_i)} = \frac{dL_r(\theta_r, \phi_r)}{L_i(\theta_i, \phi_i) d\Omega_i} \text{sr}^{-1}$$

Conservation of energy in a beam:

$$\tau + \rho + \alpha = 1$$

Kirchoff's law:

$$\alpha = \varepsilon$$

Single-surface reflectivity and transmissivity, normal incidence and no absorption:

$$\tau_{ss} = \frac{4n_1 n_2}{(n_2 + n_1)^2}; \quad \rho_{ss} = \left(\frac{n_2 - n_1}{n_2 + n_1} \right)^2$$

Internal transmittance at wavelength λ :

$$\tau_i(\lambda) = e^{-\alpha'(\lambda)x}$$

Optical thickness (optical depth) at wavelength λ :

$$\tau_o(\lambda) = \alpha'(\lambda)x$$

Equation Summary

Transmissivity, infinite number of passes:

$$\tau_{\infty} = \frac{(1 - \rho_{ss}^2)\tau_i}{1 - \rho_{ss}^2\tau_i^2}$$

Reflectivity, infinite number of passes:

$$\rho_{\infty} = \rho_{ss} + \frac{\rho_{ss}(1 - \rho_{ss})^2\tau_i^2}{1 - \rho_{ss}^2\tau_i^2}$$

Absorptivity, infinite number of passes:

$$\alpha_{\infty} = \frac{(1 - \rho_{ss})(1 - \tau_i)}{1 - \rho_{ss}\tau_i}$$

Generation of optical radiation

Planck's law:

$$L_{\lambda} = \frac{c_1}{\pi n^2 \lambda^5} \frac{1}{e^{c_2/n\lambda T} - 1}$$

Stefan-Boltzmann law:

$$M = \sigma T^4$$

Wien displacement law:

$$\lambda_{max} T = 2898 \text{ } \mu\text{m K}$$

Wien approximation:

$$L_{\lambda} = \frac{c_1}{\pi \lambda^5} e^{-\frac{c_2}{\lambda T}}$$

Rayleigh-Jeans law:

$$L_{\lambda} = \frac{2ckT}{\lambda^4}$$

Lambert-Bouguer-Beer law:

$$E_{\lambda} = E_{o\lambda} e^{-\tau_{o(\lambda)} m}$$

Equation Summary

Detectors of optical radiation

Responsivity:

$$\Re = \frac{\int R(\lambda) \Phi_{\lambda} d\lambda}{\int \Phi_{\lambda} d\lambda}$$

Signal-to-noise ratio:

$$SNR = \frac{v_s}{v_n} = \frac{i_s}{i_n}$$

Impedance:

$$Z = \frac{dV}{dI}$$

Detectivity:

$$D = \frac{1}{NEP} = \frac{SNR}{\Phi_{input}}$$

Noise equivalent power:

$$NEP = \frac{v_n}{\Re} = \Phi \frac{v_n}{v_s}$$

Specific detectivity:

$$D^* = D \sqrt{A_d B} = \frac{\sqrt{A_d B}}{NEP} = \frac{\sqrt{A_d B}}{\Phi} \frac{v_s}{v_n}$$

Specific detectivity for photons at wavelength λ :

$$D^*_q = D^* \frac{hc}{\lambda}$$

D^*_{BLIP} for a photoconductive detector:

$$D^*_{BLIP}(\lambda, f) = \lambda / 2hc \times (\eta / Eq)^{1/2}$$

D^*_{BLIP} for a photovoltaic detector:

$$D^*_{BLIP}(\lambda, f) = \sqrt{\frac{\eta \lambda}{2E_{back} hc}}$$

Equation Summary

Cutoff wavelength in micrometers:

$$\lambda_c(\mu m) = \frac{1.24}{E_g(eV)} = \frac{1.24}{\phi(eV)}$$

Photoconductive gain:

$$G = \frac{\tau_l}{\tau_{tr}}$$

Photodiode current in a photovoltaic device in the presence of incident radiation:

$$I = I_0 \left(e^{\frac{qV}{\beta kT}} - 1 \right) - I_g$$

Detector noise equations

Effective noise bandwidth:

$$B = \frac{1}{G(f_0)} \int_0^\infty G(f) df$$

Mean-square noise voltage:

$$\overline{v^2} = \overline{(v_i - v_{avg})^2} = \frac{1}{T} \int_0^T (v_i - v_{avg})^2 dt$$

Johnson noise:

$$v_j = \sqrt{4kTRB}$$

Johnson noise when B is established by an RC circuit time constant:

$$v_j = \sqrt{kT/C}$$

Shot noise:

$$i_s = \sqrt{2qI_{dc}B}$$

Equation Summary

Generation–recombination noise:

$$v_{G-R} = 2\bar{i}R \sqrt{\frac{\tau_l B}{N [1 + (2\pi f \tau_l)^2]}}$$

1/f noise:

$$i_{1/f} = \sqrt{\frac{K_s I_{dc}^\alpha B}{f^\beta}}$$

Photon noise:

$$\sqrt{(\Delta n)^2} = \sqrt{n}$$

Temperature fluctuation noise:

$$\Delta T = \sqrt{\frac{4kT^2KB}{K^2 + 4\pi^2 f^2 H^2}}$$

Quantization noise:

$$LSB = \frac{SIGNAL_{\max}}{2^n}$$

Spectrometry

Rayleigh resolution criterion:

$$\text{Resolution} = 1.22\lambda(f/\#)$$

Resolving power of a prism-based instrument:

$$Q_{rp} = b \frac{dn}{d\lambda}$$

Throughput of a prism-based instrument:

$$T = A_{slit} A_{prism} \cos \theta / f^2$$

Grating equation:

$$m\lambda = d(\sin \theta_i + \sin \theta_d)$$

Equation Summary

Resolving power of a grating-based instrument:

$$Q_{rp} = mN$$

Throughput of a grating-based instrument:

$$T = (A_{slit} A_{grating} \cos \theta) / f^2$$

Neutral density filter number:

$$n = -\log(E_{filtered}/E_{incident})$$

Radiometric calibration

Irradiance responsivity, distant small source:

$$\mathfrak{R}_E = Signal \times (d^2/I)$$

Irradiance responsivity for a distant small source used with a collimator of focal length f :

$$\mathfrak{R}_E = Signal \times (f^2/I)$$

Radiance responsivity for an extended source calibration:

$$\mathfrak{R}_L = Signal/L$$

Radiance responsivity for a near small source (Jones source) calibration:

$$\mathfrak{R}_L = Signal/L_s \times (A_o/A_s)$$

Power responsivity for direct calibration method:

$$\mathfrak{R}_\Phi = Signal/\Phi$$

Equation Summary

Measurement and range equations, NEI, and temperatures

Measurement equation for an extended source:

$$Signal = \iiint \mathcal{R}(\lambda) L_{\lambda} dA_{ap} d\Omega d\lambda$$

Measurement equation for a point source:

$$Signal = 1/d^2 \iint \mathcal{R}(\lambda) I_{\lambda} dA_{ap} d\lambda$$

Range equation:

$$R = (I_s \tau_a)^{1/2} \left[\frac{\pi}{4} \frac{D_o \tau_o}{(f/\#) \sqrt{\Omega}} \right]^{1/2} (D^*)^{1/2} \left(\frac{1}{SNR \sqrt{B}} \right)^{1/2}$$

Noise equivalent irradiance:

$$NEI = \frac{4(f/\#) \Omega^{1/2} B^{1/2}}{\pi D_o D^* \tau_o}$$

Ratio temperature:

$$\frac{L_{\lambda 1 BB}}{L_{\lambda 2 BB}} = \frac{L_{\lambda 1 unknown}}{L_{\lambda 2 unknown}}$$

Distribution temperature:

$$\int_{\lambda_1}^{\lambda_2} 1 - (M'_{\lambda} / a M_{\lambda}(T))^2 d\lambda$$

Photometry

The $V(\lambda)$ function:

$$\Phi_v = K_m \int_{380}^{760} V(\lambda) \Phi_{\lambda} d\lambda$$

The $V'(\lambda)$ function:

$$\Phi'_v = K'_m \int_{380}^{760} V'(\lambda) \Phi_{\lambda} d\lambda$$

Equation Summary

Tristimulus values:

$$\begin{aligned}
 X &= K_m \int_{380}^{760} \Phi_{\lambda} \rho(\lambda) \bar{x}(\lambda) d\lambda & Y &= K_m \int_{380}^{760} \Phi_{\lambda} \rho(\lambda) \bar{y}(\lambda) d\lambda \\
 Z &= K_m \int_{380}^{760} \Phi_{\lambda} \rho(\lambda) \bar{z}(\lambda) d\lambda
 \end{aligned}$$

References

1. P. N. Slater, *Remote Sensing: Optics and Optical Systems*, p 119, Addison–Wesley, Reading, MA, 1980.
2. F. Grum and R. J. Becherer, *Radiometry*, Vol. 1 in *Optical Radiation Measurements* series, F. Grum, Ed., p 115, Academic Press, New York (1979).
3. *Comptes Rendus de la 16^e CGPM* (16th Conférence Générale des Poids et Mesures), Resolution 3, 1979. <http://www.bipm.org/en/CGPM/db/16/3/>.
4. F. E. Nicodemus, Ed., *Self Study Manual on Optical Radiation Measurements, Part I—Concepts*, NBS Technical Note 910-1, pp 99–100, US National Bureau of Standards, Washington, DC, 1976.

Bibliography

Boyd, R. W., *Radiometry and the Detection of Optical Radiation*, John Wiley and Sons, New York (1983).

Budde, W., *Physical Detectors of Optical Radiation*, Optical Radiation Measurements, v. 4, Grum, F. and Bartleson, C. J., Eds., Academic Press, New York (1983).

Dereniak, E. L. and Crowe, D. G., *Optical Radiation Detectors*, John Wiley & Sons, New York (1984).

Dereniak, E. L. and Dereniak, T. D., *Geometrical and Trigonometric Optics*, Cambridge University Press, Cambridge, UK (2008).

Greivenkamp, J. E., *Field Guide to Geometrical Optics*, SPIE Press, Bellingham, WA (2004)
[doi:10.1117/3.547461].

Holst, G. C., *Common Sense Approach to Thermal Imaging*, JCD Publishing, Winter Park, FL, and SPIE Press, Bellingham, WA (2000).

Howell, J. R., *A Catalog of Radiation Heat Transfer Configuration Factors*.
<http://www.engr.uky.edu/rtl/Catalog/intro.html>.

NIST Physical Measurement Laboratory, *CODATA Internationally Recommended Values of the Fundamental Physical Constants*, 2006.
<http://physics.nist.gov/cuu/Constants/index.html>.

Palmer, J. M. and Grant, B. G., *The Art of Radiometry*, SPIE Press, Bellingham, WA (2009)
[doi:10.1117/3.798237].

Refractive Index.Info. <http://refractiveindex.info/>.

Robertson, A., "R2-35 Uncertainties in Distribution Temperature Determination," *Report to CIE Division 2*, Ottawa, Canada, 2005.

Vincent, J. D., *Fundamentals of Infrared Detector Operation and Testing*, John Wiley & Sons, New York (1990).

Bibliography

Wolfe, W. L. and Zissis, G. J., Eds., *The Infrared Handbook*, US Government, Washington, DC (1978), and SPIE Press, Bellingham, WA (1985).

Wyatt, C. L., *Electro-optical System Design for Information Processing*, McGraw Hill, New York (1991).

Wyatt, C. L., *Radiometric Calibration: Theory and Methods*, Academic, New York (1978).

Index

- 3-dB frequency, 49
- α/ε , 31
- A Ω product, 15
- absorptance
 - spectral, 30
 - total, 30
- absorption, 27, 30
- absorptivity, 35
- accuracy, 81
- action spectrum, 96
- airmass, 43
- Airy disk, 95
- angle
 - plane, 3
 - solid, 3
- aperture stop (AS), 21, 94
- area-solid pair, 16
- artificial sources
 - luminescent, 45
 - thermal, 45
- ASTM G-173-03 reference spectrum, 43
- background-limited
 - infrared photodetector (BLIP), 50
- baffle, 69
- bidirectional reflectance
 - distribution function (BRDF), 29
- bidirectional
 - transmittance distribution function (BTDF), 28
- blackbody radiation, 38
- bolometer, 57
- calibration
 - absolute, 73
 - distant small source, 75
 - relative, 73
- camera equation, 26
- charge transfer efficiency (CTE), 54
- charge-coupled device (CCD), 66
- charge-injection device (CID), 66
- chief ray, 94
- choppers, 68
- chopping factor, 68
- chromaticity coordinates, 87
- CIE Standard Observer, 87
- collimator, 76
 - refractive, 77
- color matching functions, 87
- color temperature, 84
- compact fluorescent lamp (CFL), 46
- complementary
 - metal-oxide semiconductor (CMOS), 66
- concise notation, 89
- conduction band, 59
- conductivity, 60
- cone, 86
- configuration factors, 19
- conservation of energy, 30
- correlated color
 - temperature (CCT), 84
- cosine correctors, 69
- cosine³ law of irradiance, 14
- cosine⁴ law of irradiance, 14

Index

- Curie temperature, 49, 58
- cutoff frequency
 - thermal, 49
- cutoff wavelength, 48, 59, 61
- depletion region, 62
- derived quantities, 6
- detector
 - area, 48
 - photon, 48
 - point, 48
 - thermal, 48
- diffraction, 95
- diffraction-limited
 - performance, 95
- direct method, 79
- distribution temperature, 84
- effective noise bandwidth (ENB), 50
- emission, 31
- emittance
 - spectral, 31
 - total, 31
- entrance pupil (NP), 94
- equation of radiative transfer, 18
- exit pupil (XP), 94
- exitance
 - radiant, 9, 10
- exposure
 - radiant, 6
- extended source
 - far, 78
 - near, 78
- external photoeffect, 61
- extrinsic semiconductors, 59
- $f/\#$
 - working, 5
- Fermi level, 59
- field lens, 22
- field stop (FS), 21, 94
- figures of merit, 51
 - D^{**} , 51
 - detective
 - quantum efficiency, 51
 - detectivity, 51
 - noise equivalent
 - power (NEP), 51
 - specific
 - detectivity, 51
- filter
 - absorption, 72
 - neutral density (ND), 72
 - thin film
 - interference, 72
- fluorescent sources, 46
- Fresnel equations, 32
- gap energy, 59
- grating, 70, 71
- grating equation, 71
- graybody, 38
- image plane irradiance, 26
- impedance, 50
- incandescent, 46
- incoherent, 18
- instantaneous field of view (IFOV), 65
- intensity, 11
 - radiant, 11
- intrinsic semiconductors, 59

Index

- invariance
 - radiance, 17
- inverse square law of
 - irradiance, 13
- irradiance, 9
- Kirchoff's law, 42
- Lambert–Bouguer–Beer
 - law, 34, 44
- Lambertian disk, 23
- Lambertian source, 12
- Lambert's law, 12
- Langley plot, 44
- laser, 47
- light-emitting diode (LED), 47
- luminous efficacy, 86
- magnification
 - pupil, 5
- marginal (rim) ray, 94
- mean-square noise
 - voltage, 52
- measurement equation, 80
- mesopic, 86
- monochromator, 70
- n*-type, 62
- natural sources
 - active, 43
 - passive, 43
- near small source (Jones source), 79
- noise, 50, 52
 - $1/f$, 53
 - amplifier, 54
 - CCD, 54
 - factor, 52
 - figure, 52
 - Generation-Recombination (G-R), 53
 - Johnson, 53
 - kT/C, 54
 - microphonic, 54
 - photon, 54
 - power, 52
 - quantization, 54
 - shot, 53
 - temperature, 52
 - temperature fluctuation, 53
 - triboelectric, 54
- noise equivalent irradiance (NEI), 83
- numerical aperture (NA), 5
- Ohm's law, 52
- optical depth, 44
- optical thickness, 34
 - spectral, 44
- order number, 71
- organic light-emitting diode (OLED), 47
- p-n* junction, 62
- p*-type, 62
- Peltier coefficient, 56
- Peltier effect, 56
- photocathode, 61
- photoconductive gain, 60
- photomultiplier tube (PMT), 61
- photon detection, 59
- photon quantities, 7
- photopic curve, 86
- photovoltaic detector, 62
- physical optics, 95

Index

- pixel, 65
- Planck's law, 38
- point source, 11
 - isotropic, 12
- potential difference, 62
- precision, 81
- prism, 70, 71
- projected area, 4
- projected solid angle, 4
- pyroelectric coefficient, 58
- pyroelectric effect, 58
- RA product, 50
- radiance, 9, 10
 - basic, 17
 - temperature, 84
- radiation
 - ionizing, 1
- radiation reference
 - source, 68
- radiation temperature, 84
- radiometry, 2
- random errors, 81
- range equation, 83
- ratio temperature, 84
- Rayleigh criterion, 70, 95
- Rayleigh-Jeans law, 40
- reflectance
 - spectral, 29
 - factor, 30
 - total, 29
- reflection, 27, 29
- reflectivity, 35
 - single-surface, 33, 35
 - specular, 32
 - total, 33
- refractive index, 2
- resolving power, 70
- responsive quantum
 - efficiency, 49
- responsivity, 48
 - irradiance, 49, 75
 - photon, 48
 - radiance, 49, 78
- reverse saturation
 - current, 63
- rod, 86
- root-mean-square (rms)
 - value, 49
- scotopic curve, 86
- Seebeck coefficient, 56
- selective radiator, 38
- signal, 50
- signal-to-noise (SNR)
 - ratio, 50
- Snell's law, 2
- solar diffusing panel, 68
- spectral absorption
 - coefficient, 34
- spectral extinction
 - coefficient, 34
- spectral instrument, 70
- spectral radiant
 - quantities, 8
- spectrometer, 70
- spectroradiometer, 70
- sphere
 - integrating, 25
 - Lambertian, 24
- Stefan-Boltzmann law, 39
- systematic errors, 81
- targets, 36
- temperature coefficient of
 - resistance (TCR), 57
- thermal conductance, 55
- thermal detection, 55

Index

- thermal resistance, 55
- thermal time constant, 55
- thermalization loss, 59
- thermoelectric effect, 56
- thermopile, 56
- throughput
 - basic, 15
- time constant
 - thermal, 49
- transit time, 60
- transmission, 27, 28
- transmissivity, 35
 - single-surface, 33, 35
 - specular, 32
 - total, 33
- transmittance, 44
 - internal, 34, 35
 - spectral, 28
 - total, 28
- tristimulus values, 87
- uncertainty
 - absolute, 89
 - relative, 89
- valence band, 59
- velocity of light, 2
- velocity of propagation, 2
- Wien approximation, 40
- Wien displacement law
 - (Wien's law), 39, 41
- work function, 61



Barbara G. Grant received her B.A. in mathematics from San Jose State University in 1983, and her M.S. in optical sciences from the University of Arizona in 1989, where her graduate research focused on the absolute radiometric calibration of spaceborne imaging sensors. She was employed in the aerospace and defense industry prior to attending the University of Arizona and afterward, working at companies such as Lockheed Missiles and Space and NASA contractors. She received two NASA Group Achievement Awards for her work on the GOES imager and sounder.

In 1994 Grant began her consultancy, Lines and Lights Technology, which provides consulting and training in diverse applications of electro-optical technology including infrared sensors, UV measurement, and systems engineering/systems analysis. Barbara enjoys teaching and has taught several short courses for SPIE and in other venues. She has been interviewed on technical subjects for print and Internet media, and has appeared on radio and television. In December 2009, she completed *The Art of Radiometry* (SPIE Press) as co-author to the late Jim Palmer, who had mentored her in the subject for many years.